Inorg. Chem. **2007**, *46*, 10093–10107

$[Cr^{III}(NCMe)_6]^{3+}$—a Labile Cr^{III} Source Enabling Formation of $Cr[M(CN)_6]$ (M = V, Cr, Mn, Fe) Prussian Blue-Type Magnetic Materials

Kendric J. Nelson,[†] Matthew C. Daniels,[†] William M. Reiff,[‡] Shayla A. Troff,[†] and Joel S. Miller*,[†]

Department of Chemistry, University of Utah, 315 South 1400 East, Room 2020, Salt Lake City, Utah 84112-0850, and Department of Chemistry and Chemical Biology, Northeastern University, 9 Hurtig Hall, Boston, Massachusetts 02115

Received May 2, 2007

The kinetic inertness of the hexaaquachromium(III) (k_{H_2O}= 2.4×10^{-6} s^{-1}) has led to challenges with respect to incorporating Cr^{III} ions into Prussian blue-type materials; however, hexakis(acetonitrile)chromium(III) was shown to be substantially more labile ($\sim 10^4$ times) and enables a new synthetic route for the synthesis of these materials via nonaqueous solvents. The synthesis, spectroscopic, and physical properties of $Cr[M(CN)_6]$ (M = V, Cr, Mn, Fe) Prussian blue analogues synthesized from $[Cr^{III}(NCMe)_6]^{3+}$ and the corresponding $[M^{III}(CN)_6]^{3-}$ are described. All these compounds $\{(NEt_4)_{0.02}Cr^{III}[V^{III}(CN)_6]_{0.98}(BF_4)_{0.08}\cdot 0.10MeCN$ (**1**), $Cr^{III}[Cr^{III}(CN)_6]\cdot 0.16MeCN$ (**2**), $Cr^{III}[Mn^{III}(CN)_6]\cdot 0.10MeCN$ (**3**), and $(NEt_4)_{0.04}Cr^{III}_{0.64}Cr^{IV}_{0.40}[Fe^{II}(CN)_6]_{0.40}[Fe^{III}(CN)_6]_{0.60}(BF_4)_{0.16}\cdot 1.02MeCN$ (**4**)$\}$ are ferrimagnets exhibiting cluster-glass behavior. Strong antiferromagnetic coupling was observed for M = V, Cr, and Mn with Weiss constants (θ) ranging from –132 to –524 K; and in **2**, where the strongest coupling is observed (θ = –524 K), the highest T_c (110 K) value was observed. Weak antiferromagnetic coupling was observed for M = Fe (θ = –12 K) leading to the lowest T_c (3 K) value in this series. Weak coupling and the low T_c value observed in **4** were additionally contributed by the presence of both $[Fe^{II}(CN)_6]^{4-}$ and $[Fe^{III}(CN)_6]^{3-}$ as confirmed by ^{57}Fe–Mössbauer spectroscopy.

Introduction

Prussian blue materials are of increasing focus for the design and synthesis of new molecule-based magnets (MBMs).[1] MBMs have potential uses in many areas including magnetic shielding[2] and spintronic memory storage devices.[3] Prussian blue analogues (PBAs) are synthesized by reacting $[M(solvent)_x]^{n+}$ with $[M'(CN)_6]^{m-}$ to form $A_aM_b[M'(CN)_6]_c\cdot z(solvent)$ that adopts a face-centered cubic (fcc) structure.[1,4] Due to the use of the $[M(solvent)_x]^{n+}$ and $[M'(CN)_6]^{m-}$ molecule-based building blocks, PBAs can be easily tailored to possess numerous metal ions that vary in charge and number of spins per metal site and thus can lead to a variety of magnetic behaviors. Ultimately, it is desirable to obtain high-critical-temperature (T_c) magnetic materials that order near or above room temperature. Examples of high-T_c Prussian blue magnets include $Cr^{II}_{1.5}[Cr^{III}(CN)_6]\cdot 5H_2O$ (T_c

* To whom correspondence should be addressed. E-mail: jsmiller@chem.utah.edu.
[†] University of Utah.
[‡] Northeastern University.

(1) Verdaguer, M.; Girolami, G. S. In *Magnetism—Molecules to Materials*; Miller, J. S., Drillon, M., Eds.; Wiley-VCH: Weinheim, Germany, 2005; Vol. 5, pp 283−346.
(2) Morin, B. G.; Hahm, C.; Epstein, A. J.; Miller, J. S. *J. Appl. Phys.* **1994**, *75*, 5782. Miller, J. S. *Adv. Mater.* **1994**, *6*, 322. Landee, C. P.; Melville, D.; Miller, J. S. In *NATO ARW Molecular Magnetic Materials*; Kahn, O., Gatteschi, D., Miller, J. S., Palacio, F., Eds.; Kluwer Academic Publishers: London, 1991; Vol. E198, p 395.
(3) Prigodin, V. N.; Raju, N. P.; Pokhodnya, K. I.; Miller, J. S.; Epstein, A. J. *Adv. Mater.* **2002**, *14*, 1230.
(4) Ludi, A.; Güdel, H. U. *Struct. Bonding* **1973**, *14*, 1. Dunbar, K. R.; Heintz, R. A. *Prog. Inorg. Chem.* **1997**, *45*, 283.
(5) Mallah, T.; Thiébaut, S.; Verdaguer, M.; Veillet, P. *Science* **1993**, *262*, 1554.
(6) Buschmann, W. E.; Paulson, S. C.; Wynn, C. M.; Girtu, M.; Epstein, A. J.; White, H. S.; Miller, J. S. *Adv. Mater.* **1997**, *9*, 645. Buschmann, W. E.; Paulson, S. C.; Wynn, C. M.; Girtu, M.; Epstein, A. J.; White, H. S.; Miller, J. S. *Chem. Mater.* **1998**, *10*, 1386.
(7) (a) Ferlay, S.; Mallah, T.; Ouahes, R.; Veillet, P.; Verdaguer, M. *Nature* **1995**, *378*, 701. (b) Dujardin, E.; Ferlay, S.; Phan, X.; Desplanches, C.; Moulin, C. C. D.; Sainctavit, P.; Baudelet, F.; Dartyge, E.; Veillet, P.; Verdaguer, M. *J. Am. Chem. Soc.* **1998**, *120*, 11347. (c) Ferlay, S.; Mallah, T.; Ouahes, R.; Veillet, P.; Verdaguer, M. *Inorg. Chem.* **1999**, *38*, 229. (d) Verdaguer, M.; Bleuzen, A.; Marvaud, V.; Vaissermann, J.; Seuleiman, M.; Desplanches, C.; Scuiller, A.; Train, C.; Garde, R.; Gelly, G.; Lomenech, C.; Rosenman, I.; Veillet, P.; Cartier, C.; Villain, F. *Coord. Chem. Rev.* **1999**, *190−192*, 1023. (e) Verdaguer, M.; Bleuzen, A.; Train, C.; Garde, R.; Fabrizi de Biani, F.; Desplanches, C. *Philos. Trans. R. Soc. London, Ser. A* **1999**, *357*, 2959. (f) K. Hashimoto, S. Ohkoshi, *Philos. Trans. R. Soc. London, Ser. A* **1999**, *357*, 2977.

10.1021/ic7008489 CCC: $37.00
Published on Web 10/24/2007

= 240 K),[5] $Cr^{III}[Cr^{III}(CN)_6]_{0.93}[Cr^{II}(CN)_6]_{0.05}$ (T_c = 260 K),[6] and several vanadium hexacyanochromate room-temperature magnets: $V^{II}_{0.42}V^{III}_{0.58}[Cr^{III}(CN)_6]_{0.86}\cdot 2.8H_2O$ (T_c = 315 K),[7a] $V^{II}_{0.45}V^{III}_{0.53}(V^{IV}O)_{0.02}[Cr^{III}CN)_6]_{0.69}(SO_4)_{0.23}\cdot 3.0H_2O\cdot 0.02K_2SO_4$ (T_c = 310 K),[7b] and $Cs_{0.82}V^{II}_{0.66}(V^{IV}O)_{0.34}Cr^{III}(CN)_6]_{0.92}(SO_4)_{0.203}\cdot 3.6H_2O$ (T_c = 315 K)[7b] reported by Verdaguer and co-workers. Subsequently, $K_{0.50}V^{II}_{0.65}V^{III}_{0.35}[Cr(CN)_6]_{0.95}\cdot 1.7H_2O$ (T_c = 350 K),[8a] as well as $KV^{II}[Cr^{III}(CN)_6]\cdot 2H_2O\cdot 0.1KO_3SCF_3$[8b] and $K_{0.058}V^{II}_{0.57}V^{III}_{0.43}[Cr^{III}(CN)_6]_{0.79}\cdot (SO_4)_{0.058}\cdot 0.93H_2O$[8a] with a similar T_c (~100 °C) were reported.

The use of $[Cr^{III}(solvent)_6]^{3+}$ as the solvated metal cation building block has been a challenge in the synthesis of PBAs due to its kinetic inertness to ligand substitution. For example, $[Cr^{III}(OH_2)_6]^{3+}$ has long been known to be substitutionally inert ($k_{H_2O} = 2.4 \times 10^{-6}$ s^{-1}),[9] and attempts to react it with $[M'(CN)_6]^{m-}$ to produce PBAs have proven fruitless.[10] Although this posed a synthetic challenge to incorporate Cr^{III} into the nitrogen end of the cyanide in PBAs, $Cr^{III}-N\equiv C-M'$, there have been reports of this binding motif. For example, iron(II) hexacyanochromate(III) can be transformed into the more stable chromium(III) hexacyanoferrate(II) thermally,[11] electrochemically,[12] and by pressure-inducement.[13] Chromium(III) bound to the nitrogen of the cyanide bridging ligand has also been reported in several chromium cyanide species prepared by the traditional solution route[5] as well as electrochemically.[14] We have also reported the formation of $Cr^{III}-N\equiv C-M'$ linkages from electron transfer occurring in the solid state. This results in the formation of $Cr^{III}-N\equiv C-Mn^{III}$ linkages in $Cr^{III}[Mn^{III}(CN)_6]$[15] and $Cr^{III}-N\equiv C-V^{II}$ linkages in $Cr^{II}_{0.5}Cr^{III}[V^{II}(CN)_6]\cdot zMeCN$.[16] The latter is formed by reacting $[Cr^{II}(NCMe)_4]^{2+}$ with $[V^{III}(CN)_6]^{3-}$ (3:2) in MeCN and exhibits an unique solvent dependency of the structural and magnetic properties. In the former case, $[Cr^{II}(NCMe)_6]^{2+}$ is mixed with $[Mn^{IV}(CN)_6]^{2-}$ (1:1) in nonaqueous media, and electron transfer occurs from Cr^{II} to Mn^{IV} resulting in the $Cr^{III}[Mn^{III}(CN)_6]$ PBA. This material exhibits ferrimagnetic ordering with a T_c value of 16 K and a coercive field, H_{cr}, of 130 Oe at 5 K.[16]

$[Cr^{III}(NCMe)_6](BF_4)_3$ has recently been reported to be a nonaqueous source of Cr^{III};[17] we report herein that $[Cr^{III}(NCMe)_6]^{3+}$ is substitutionally more labile than the kinetically inert $[Cr^{III}(OH_2)_6]^{3+}$, and the reaction with $[M(CN)_6]^{3-}$ (M = V^{III}, Cr^{III}, Mn^{III}, Fe^{III}) results in the formation of new PBAs.

Experimental Section

All manipulations were carried out under a dry N_2 atmosphere (<1 ppm O_2) using Schlenck techniques or in a Vacuum Atmospheres DriLab. $(NEt_4)_3[V^{III}(CN)_6]$,[16] $(NEt_4)_3[M(CN)_6]$ (M = Cr^{III}, Fe^{III}),[18] $(NEt_4)_3[Mn^{III}(CN)_6]$,[19] and $[Cr^{III}(NCMe)_6](BF_4)_3$[17] were prepared via literature routes. Acetonitrile (MeCN) was purified through an activated alumina dual column purification system under a positive pressure of N_2, while diethyl ether (Et_2O) was purified via distillation under positive dry N_2 pressure using sodium dispersion (Strem) and benzophenone (Lancaster). Deionized water was deoxygenated by distillation over $KMnO_4$ under positive N_2 pressure.

Physical Methods. Infrared spectra were recorded from 400 to 4000 cm^{-1} on a Bruker Tensor 37 infrared spectrophotometer (±1 cm^{-1}) as either KBr pellets or Nujol mulls between NaCl salt plates. Electronic absorption spectra were recorded from 10 000 to 50 000 cm^{-1} on an Ocean Optics HR2000 spectrophotometer equipped with fiber-optic cables fed through the wall of a Vacuum Atmospheres DriLab apparatus under an inert atmosphere and were taken in a 1.00 cm quartz cuvette.

Centrifugation of samples was performed using a Clay Adams centrifuge with a fixed rotary speed of 3200 rpm. Samples were centrifuged for 10 min to separate the solid precipitates from the mother liquor.

Thermogravimetric analyses coupled with mass spectroscopy (TGA/MS) measurements were performed on a TA Instruments Model 2050 TGA analyzer coupled to a Thermolab TL1285 thermal analysis−mass spectrometer. The TGA operates between ambient temperature and 1000 °C and was located in a Vacuum Atmospheres DriLab apparatus under an inert atmosphere. TGA samples were handled in a nitrogen atmosphere and heated under a nitrogen purge. Heating rates were 5 °C/min. Elemental analyses were performed by GCL & Chemisar Laboratories (Guelph, Ontario, Canada) on freshly prepared samples that were sealed under a dry N_2 atmosphere and sent off for analysis.

Powder X-ray diffraction (PXRD) scans were obtained on a $\theta\angle\theta$ Bruker AXS D8 Avance diffractometer (2θ of 12.5° to 42.5°, step width of 0.02°, counting time of 10 s/step, voltage of 40 kV, and current of 40 mA) fitted with a Göbel mirror to remove all but the Cu Kα radiation (λ = 1.54060 Å). Samples were sealed under inert atmosphere in 1.00 mm thin-walled quartz capillaries to prevent oxidation/moisture absorption, and scans were performed at room temperature (~298 K).

Samples used for ^{57}Fe−Mössbauer studies were enclosed in a nylon holder that was sealed with epoxy. The spectra were determined by using a conventional constant-acceleration spectrometer operated in multichannel scaling mode. The γ-ray source consisted of a fresh 25 mCi portion of ^{57}Co in a rhodium metal matrix that was maintained at ambient temperature. The spectrom-

(8) (a) Hatlevik, Ø.; Buschmann, W. E.; Zhang, J.; Manson, J. L.; Miller, J. S. *Adv. Mater.* **1999**, *11*, 914. (b) Holmes, S. M.; Girolami, G. S. *J. Am. Chem. Soc.* **1999**, *121*, 5593.

(9) (a) Swaddle, T. W. *Coord. Chem. Rev.* **1974**, *14*, 217. (b) Prasad, D.-R.; Ramasami, T.; Ramaswamy, D.; Santappa, M. *Inorg. Chem.* **1980**, *19*, 3181. (c) Xu, F.-C.; Krouse, H. R.; Swaddle, T.W. *Inorg. Chem.* **1985**, *24*, 267. (d) Lincoln, S. F. *Helv. Chim. Acta* **2005**, *88*, 523.

(10) Sato, O.; Gu. Z.; Etoh, H.; Ichiyanagi, J.; Iyoda, T.; Fujishima, A.; Hashimoto, K. *Chem. Lett.* **1997**, 37.

(11) (a) Shriver, D. F.; Shriver, S. A.; Anderson, S. E. *Inorg. Chem.* **1965**, *4*, 725. (b) Brown, D. B.; Shriver, D. F.; Schwartz, L. H. *Inorg. Chem.* **1968**, *7*, 77. (c) House, J. E., Jr.; Bailar, J. C., Jr. *Inorg. Chem.* **1969**, *8*, 672. (d) Reguera, E;, Bertrán, J. F.; Nuñez, l. *Polyhedron* **1994**, *13*, 1619.

(12) Dostal, A.; Schröder, U.; Scholz, F. *Inorg. Chem.* **1995**, *34*, 1711.

(13) Coronado, E.; Giménez-López, M. C.; Levchenko, G.; Romero, F. M.; García-Baonza, V.; Milner, A.; Paz-Pasternak, M. *J. Am. Chem. Soc.* **2005**, *127*, 4580.

(14) (a) Sato, O.; Iyoda, T.; Fujishima, A.; Hashimoto, K. *Science* **1996**, *271*, 49. (b) Sato, O.; Gu, Z.; Etoh, H.; Ichiyanagi, J.; Iyoda, T.; Fujishima, A.; Hashimoto, K. *Chem. Lett.* **1997**, 37.

(15) Buschmann, W. E.; Miller, J. S. *Inorg. Chem.* **2000**, *39*, 2411.

(16) Nelson, K. J.; Giles, I. D.; Troff, S. A.; Arif, A. M.; Miller, J. S. *Inorg. Chem.* **2006**, *45*, 8922.

(17) Hatlevik, Ø.; Arif, A. M.; Miller, J. S. *J. Phys. Chem. Solids* **2004**, *65*, 61.

(18) Le Maguerès, P.; Ouahab, L.; Briard, P.; Even, J.; Bertault, M.; Toupet, L.; Rámos, J.; Gómez-García, C. J.; Delhaès, P. *Mol. Cryst. Liq. Cryst.* **1997**, *305*, 479.

(19) Gritzner, G.; Danksagmüller, K.; Gutmann, V. *J. Electroanal. Chem.* **1978**, *90*, 203.

eter was calibrated using a 6 μm thick natural-abundance iron foil. Isomer shifts are reported relative to the center of the magnetic hyperfine pattern of the latter foil taken as zero velocity. The linewidths of the innermost pair of the $\Delta M = \pm 1$ transitions of the latter Zeeman pattern were reproducibly determined to be 0.230 mm/s. Sample temperature control was achieved using a standard exchange gas liquid helium cryostat (Cryo Industries of America, Inc.) with temperature measurement and control based on silicon diode thermometry in conjunction with a 10 μA excitation source (Lakeshore Cryotronics, Inc.). Spectra were fit to unconstrained Lorentzians using the program *ORIGIN* (Origin Lab, Inc.).

Magnetic susceptibility measurements were made between 2 and 300 K using a Quantum Design MPMS-5 5T SQUID magnetometer with a sensitivity of 10^{-8} or 10^{-12} emu/Oe at 1 T and equipped with the ultralow field ($\sim$0.005 Oe), reciprocating sample measurement system, and continuous low-temperature control with enhanced thermometry features or using a Quantum Design PPMS-9 ac/dc susceptometer. Measurements were made on powders contained in airtight Delrin holders supplied by Quantum Design. Small amounts of quartz wool were used in the Delrin holders to minimize the movement of the powders during measurements. The data were corrected for the measured diamagnetism of each holder, and core diamagnetic corrections of -105, -104, -102, and -137×10^{-6} emu/mol were calculated from Pascal's constants for complexes **1**, **2**, **3**, and **4**, respectively.

Lability Studies of $[Cr^{III}(NCMe)_6]^{3+}$ in MeCN. $[Cr^{III}(NCMe)_6](BF_4)_3$ (73.40 mg, 0.1314 mmol) was dissolved in 5.00 mL of MeCN resulting in a 26.27 mM Cr^{III} solution, and 150 μL of deoxygenated H_2O was added to 1.50 mL of this 26.27 mM Cr^{III} solution in a 1.00 cm quartz cell and was immediately mixed via shaking. At the same time the H_2O was added to the Cr^{III} solution, a time acquisition UV$-$vis experiment was initiated and spectra were taken at 10 s intervals. Immediately upon the addition of H_2O to the Cr^{III} solution, a drastic change in the UV$-$vis spectrum was observed as the $[Cr^{III}(NCMe)_6]^{3+}$ absorption bands (27 322 and 20 243 cm^{-1}) began to decrease in intensity and bands corresponding to $[Cr^{III}(OH_2)_6]^{3+}$ (24 631 and 17 483 cm^{-1}) simultaneously grew in (Figure S1, Supporting Information). The conversion of $[Cr^{III}(NCMe)_6]^{3+}$ to $[Cr^{III}(OH_2)_6]^{3+}$ appeared to be complete in less than a minute.

$(NEt_4)_{0.02}Cr[V(CN)_6]_{0.98}(BF_4)_{0.08}\cdot 0.10MeCN$, 1. Compound **1** was synthesized by slowly adding a 10 mL MeCN solution of $(NEt_4)_3[V^{III}(CN)_6]$ (144.0 mg, 0.2405 mmol, 1.00 equiv) via a syringe pump at 2 mL/h into a stirring 20 mL MeCN solution of $[Cr^{III}(NCMe)_6](BF_4)_3$ (134.4 mg, 0.2405 mmol, 1.00 equiv). This immediately formed a dark brown precipitate. After the complete addition of the V^{III} solution, the mixture was stirred for approximately 30 min. The dark brown product was collected via centrifugation, the colorless supernate was decanted, and the product was washed with MeCN (3×15 mL), followed by 15 mL of Et_2O, and dried at room temperature under vacuum for 12 h. A dark brown solid was isolated in quantitative yield. Anal. Calcd for $(NEt_4)_{0.02}Cr[V(CN)_6]_{0.98}(BF_4)_{0.08}\cdot 0.10MeCN$, $C_{6.24}H_{0.70}N_{6.00}B_{0.08}Cr_{1.00}F_{0.32}V_{0.98}$: C, 27.91; H, 0.26; N, 31.29; V, 18.59; Cr, 19.36. Found: C, 27.10; H, 1.72; N, 31.55; V, 19.24; Cr, 19.21.[20] TGA/MS analysis (vide infra) showed that the sample was thermally unstable at relatively low temperatures (40 °C) above which solvent loss and decomposition occured simultaneously (Figure S2, Supporting Information). IR ν_{CN} (KBr): 2136 (s) cm^{-1} (half-width at half-height (hwhh): 52 cm^{-1}).

$Cr[Cr(CN)_6]\cdot 0.16MeCN$, 2. Compound **2** was synthesized by slowly adding a 10 mL MeCN solution of $(NEt_4)_3[Cr^{III}(CN)_6]$ (153.3 mg, 0.2560 mmol, 1.00 equiv) via a syringe pump at 2 mL/h into a stirring 20 mL MeCN solution of $[Cr^{III}(NCMe)_6](BF_4)_3$ (142.7 mg, 0.2554 mmol, 1.00 equiv). This immediately formed a red-brown precipitate. After complete addition of the Cr^{III} solution, the mixture was stirred for approximately 30 min. The red-brown product was collected via centrifugation while the colorless supernate was decanted. The product was washed with MeCN (3×15 mL), followed by 15 mL of Et_2O and dried at room temperature under vacuum for 12 h. A red-brown solid was isolated in a quantitative yield. Anal. Calcd for $Cr[Cr(CN)_6]\cdot 0.16MeCN$, $C_{6.32}H_{0.48}N_{6.16}Cr_{2.00}$: C, 28.47; H, 0.18; N, 32.36; Cr, 39.00. Found: C, 27.07; H, 1.01; N, 31.80; Cr, 38.04.[20] TGA/MS analysis (vide infra) showed the sample was thermally unstable at relatively low temperatures (40 °C) above which solvent loss and decomposition occur simultaneously (Figure S2, Supporting Information). IR ν_{CN} (KBr): 2173 (s) (hwhh: 26 cm^{-1}) and $\sim$2120 (w, shoulder) cm^{-1}.

$Cr[Mn(CN)_6]\cdot 0.10MeCN$, 3. Compound **3** was synthesized by slowly adding a 10 mL MeCN solution of $(NEt_4)_3[Mn^{III}(CN)_6]$ (120.0 mg, 0.2028 mmol, 1.00 equiv) via a syringe pump at 2 mL/h into a stirring 20 mL MeCN solution of $[Cr^{III}(NCMe)_6](BF_4)_3$ (113.3 mg, 0.2028 mmol, 1.00 equiv). This formed an immediate dark brown precipitate. After complete addition of the Mn^{III} solution, the mixture was stirred for approximately 30 min. The dark brown product was collected via centrifugation, the colorless supernate was decanted product was washed with MeCN (3×15 mL), followed by 15 mL of Et_2O and dried at room temperature under vacuum for 12 h. A dark brown solid was isolated in a quantitative yield. Anal. Calcd for $Cr[Mn(CN)_6]\cdot 0.10MeCN$, $C_{6.20}H_{0.30}N_{6.10}Cr_{1.00}Mn_{1.00}$: C, 27.88; H, 0.11; N, 31.98; Cr, 19.46; Mn, 20.56. Found: C, 27.59; H, 1.01; N, 32.28; Cr, 20.37; Mn, 19.71.[20] TGA/MS analysis (vide infra) showed that the sample was thermally unstable at relatively low temperatures (40 °C) above which solvent loss and decomposition occur simultaneously (Figure S2, Supporting Information). IR ν_{CN} (KBr): 2144 (s) cm^{-1} (hwhh: 39 cm^{-1}).

$(NEt_4)_{0.04}Cr_{1.04}[Fe(CN)_6](BF_4)_{0.16}\cdot 1.02MeCN$, 4. Compound **4** was synthesized by slowly adding a 10 mL MeCN solution of $(NEt_4)_3[Fe^{III}(CN)_6]$ (116.8 mg, 0.1938 mmol, 1.00 equiv) via a syringe pump at 2 mL/h into a stirring 20 mL MeCN solution of $[Cr^{III}(NCMe)_6](BF_4)_3$ (108.3 mg, 0.1938 mmol, 1.00 equiv). This formed an immediate dark red-brown precipitate. After complete addition of the Fe^{III} solution, the mixture was stirred for approximately 30 min. The dark red-brown product was collected via centrifugation, the colorless supernate was decanted. The product was washed with MeCN (3×15 mL), followed by 15 mL of Et_2O and dried at room temperature under vacuum for 12 h. A dark brown solid was isolated in quantitative yield. Anal. Calcd for $(NEt_4)_{0.04}Cr_{1.04}[Fe(CN)_6](BF_4)_{0.16}\cdot 1.02MeCN$, $C_{8.36}H_{3.86}N_{7.06}B_{0.16}Cr_{1.04}F_{0.64}Fe_{1.00}$: C, 30.71; H, 1.19; N, 30.24; Cr, 16.54; Fe, 17.08. Found: C, 30.31; H, 1.59; N, 30.48; Cr, 16.48; Fe, 16.68.[20] TGA/MS analysis (vide infra) showed that the sample was thermally unstable at relatively low temperatures (40 °C) above which solvent loss and decomposition occur simultaneously (Figure S2, Supporting Information). IR ν_{CN} (Nujol): 2143 (s) (hwhh: 31 cm^{-1}) and 2096 (s) cm^{-1} (hwhh: 29 cm^{-1}).

Results and Discussion

Lability of $[Cr^{III}(NCMe)_6]^{3+}$ in MeCN. The lability of $[Cr^{III}(NCMe)_6]^{3+}$ was experimentally observed by the addition of water while simultaneously monitoring the formation

(20) The thermal instability likely contributes to the deviations in the elemental analyses data, and therefore, a larger tolerance was allowed in fitting the chemical composition.

of $[Cr^{III}(OH_2)_6]^{3+}$ (eq 1) as a function of time via UV−vis spectroscopy. Upon the addition of 150 μL of H_2O to a 1.50 mL orange-colored MeCN solution of 26.27 mM $[Cr^{III}(NCMe)_6](BF_4)_3$, the 27 322 and 20 243 cm^{-1} absorption bands for $[Cr^{III}(NCMe)_6]^{3+}$ [17] began to decrease in intensity, and bands at 24 631 and 17 483 cm^{-1}, corresponding to $[Cr^{III}(OH_2)_6]^{3+}$, simultaneously grew in with the solution color changing to light green (Figure S1, Supporting Information).[21] The reaction appeared to be complete in less than 60 s with no further change in the electronic spectrum. The rate law for this reaction is represented in eq 2.

$$[Cr^{III}(NCMe)_6]^{3+} + H_2O \xrightarrow{k_1} [Cr^{III}(OH_2)_6]^{3+} \quad (1)$$

$$\text{rate} = \frac{-d[[Cr^{III}(NCMe)_6]^{3+}]}{dt} = k_1[[Cr^{III}(NCMe)_6]^{3+}][H_2O] \quad (2)$$

Since $[H_2O] \gg [[Cr^{III}(OH_2)_6]^{3+}]$, the rate law can be simplified into pseudo-first-order conditions resulting in

$$k_{obs} = k_1[H_2O] \quad (3)$$

$$\text{rate} = \frac{-d[[Cr^{III}(NCMe)_6]^{3+}]}{dt} = k_{obs}[[Cr^{III}(NCMe)_6]^{3+}] \quad (4)$$

and by rearranging and integrating, the rate law becomes eq 5.

$$\ln[[Cr^{III}(NCMe)_6]^{3+}] = \ln[[Cr^{III}(NCMe)_6]^{3+}]_0 - k_{obs}t \quad (5)$$

By plotting $\ln[[Cr^{III}(NCMe)_6]^{3+}]$ vs t, the observed rate constant (k_{obs}) for this MeCN substitution by water was estimated to be 2.7×10^{-2} s^{-1} from the slope of this plot (Figure S1 inset, Supporting Information). Thus, the overall rate of ligand substitution for $[Cr^{III}(NCMe)_6]^{3+}$ is $\sim 10^4$ faster than for the kinetically inert $[Cr^{III}(OH_2)_6]^{3+}$ (2.4×10^{-6} s^{-1}).[9] Therefore, $[Cr^{III}(NCMe)_6]^{3+}$ is a nonaqueous Cr^{III} source that can be useful in the design and synthesis of new PBAs.

Synthesis. Formation of $Cr^{III}[M(CN)_6]$ (M = V, Cr, Mn,[22] Fe) has been thwarted due to the lack of a suitable labile source of Cr^{III}; however, with the advent of $[Cr^{III}(NCMe)_6](BF_4)_3$,[17] these materials were targeted for preparation via the slow addition of stoichiometric amounts of the corresponding $(NEt_4)_3[M^{III}(CN)_6]$. The slow, controlled addition was achieved by a syringe pump addition. All of these deeply colored solids are quite moisture-sensitive and were handled under a dry N_2 atmosphere. The only sample that was additionally extremely air-sensitive was the vanadium-containing material, which was again handled under a dry N_2 atmosphere at all times to avoid oxidation. The compositions of these materials were determined by elemental[23] and thermogravimetric analyses, and the assignments of oxidation states were concluded from stoichiometry as well as infrared studies for M = V, Cr, Mn, and Fe and ^{57}Fe−Mössbauer spectroscopy for M = Fe. We believe that this problem in part result from the thermal instability of these phases slightly above room temperature (vide infra). Therefore, somewhat larger errors in the atom percentages were accepted in order to obtain compounds that made chemical sense, stoichiometrically.

Table 1. Characteristic IR ν_{CN} Absorptions and Colors of $Cr[M(CN)_6]$ (M = V, Cr, Mn, Fe)

M	color	ν_{CN} (cm^{-1})	ν_{CN} (cm^{-1}), $(NEt_4)_3[M^{III}(CN)_6]$	$\Delta\nu_{CN}$ (cm^{-1})[a]
V	dark brown	2136	2107	29
Cr	red-brown	2173	2111	62
Mn	dark brown	2144	2097	47
Fe	dark red-brown	2096, 2143	2097	−1, 46

[a] $\Delta\nu_{CN}$ is the shift in the ν_{CN} absorption with respect to the parent cyanometalate complex upon binding to Cr, forming $Cr[M(CN)_6]$.

Infrared Spectra. $Cr[M(CN)_6]$ (M = V, Cr, Mn) exhibit broad, single ν_{CN} absorptions between 2136 and 2173 cm^{-1} (Table 1, Figure S3, Supporting Information), which are shifted to higher frequencies with respect to the corresponding isolated $[M(CN)_6]^{3-}$ parent compounds. This shift is consistent with that of other PBAs and is due to the loss of electron density from the 5σ orbital and the lack of back-bonding via the N atom.[24] Thus, the carbon-bound M atom is in the same oxidation state as the building block, and for $Cr[M(CN)_6]$ (M = V, Cr, Mn), $Cr^{III}-N\equiv C-M^{III}$ linkages are confirmed. These materials are formulated as $(NEt_4)_{0.02}Cr^{III}[V^{III}(CN)_6]_{0.98}(BF_4)_{0.08}\cdot 0.10MeCN$ (**1**), $Cr^{III}[Cr^{III}(CN)_6]\cdot 0.16MeCN$ (**2**), and $Cr^{III}[Mn^{III}(CN)_6]\cdot 0.10MeCN$ (**3**). Compound **1** is the first example of a $[V^{III}(CN)_6]^{3-}$-based PBA and therefore is the first example of a material containing $M-N\equiv C-V^{III}$ linkages (M = Cr^{III} for **1**). The possibility of linkage isomerization to form $Cr^{III}-C\equiv N-V^{III}$ binding motifs was considered; however, the ν_{CN} absorptions in the high-T_c materials where $Cr^{III}-C\equiv N-V^{II/III}$ linkages are present were well-characterized with a typical absorption value of 2111 ± 7 cm^{-1}.[7,8] In **2**, a ν_{CN} absorption of 2173 cm^{-1} was observed, which is consistent with previously prepared PBAs containing $Cr^{II/III}-N\equiv C-Cr^{III}$ linkages (2185−2194 cm^{-1}).[5,6,14] The IR spectrum of **3** is virtually identical to that of the material formed when $[Cr^{II}(NCMe)_6]^{2+}$ was reacted with $[Mn^{IV}(CN)_6]^{2-}$, as a subsequent electron transfer occurred.[15] The IR spectrum of this previous compound has a ν_{CN} at 2137 cm^{-1} (hwhh = 14 cm^{-1}), and in **3** the ν_{CN} is $\sim$2144 cm^{-1} (hwhh = 39 cm^{-1}); thus, both samples have $Cr^{III}-N\equiv C-Mn^{III}$ linkages. The larger hwhh value suggests that **3** is more structurally disordered than the sample previously prepared in ref 15.

(21) Figgis, B. N.; Hitchman, M. A. *Ligand Field Theory and Its Applications*; Wiley-VCH: New York, 2000, 207. In water, Cr^{III} salts are light green in color with absorption bands at 17 000 and 24 000 cm^{-1}. The difference in our observed absorption bands at 24 631 and 17 483 cm^{-1} and those reported in the literature is likely shifted due to the spectra being measured in MeCN in our experiments.

(22) Previously, $Cr^{III}[Mn^{III}(CN)_6]$ has been indirectly synthesized from the stoichiometric reaction of $[Cr^{II}(NCMe)_6]^{2+}$ and $[Mn^{IV}(CN)_6]^{2-}$ in CH_2Cl_2,[15] where electron transfer occurs. However, in the preparation reported here, no electron transfer is needed to obtain the product.

(23) Miller, J. S.; Kravitz, S. H; Kirschner, S.; Ostrowski, P.; Nigrey, P. J. *J. Chem. Ed.* **1978**, *55*, 181.

(24) Nakamoto, K. In *Infrared and Raman Spectra of Inorganic and Coordination Compounds Part B: Applications in Coordination, Organometallic, and Bioinorganic Chemistry*, 5th ed.; Wiley-Interscience: New York, 1997; p 111.

Materials **1**−**3** also have a small amount of both coordinated (ν_{CN} = 2298 and 2325 cm^{-1}) and noncoordinating MeCN (ν_{CN} = 2252 cm^{-1}). Upon exposure to air, these absorptions rapidly disappear and a simultaneous growth of ν_{OH} absorptions is observed. This also occurs for $[Cr^{III}(NCMe)_6](BF_4)_3$.[17] Thus, MeCN can be easily displaced by water upon exposure to moisture, and it is likely that the MeCN in these materials is on the surface and/or in the interstitial lattice sites, as previously reported.[15] The IR spectra also show trace amounts of NEt_4^+ and BF_4^- that was minimized but not eliminated by thoroughly washing the solids with MeCN. The samples chosen for analyses were verified to have minimal amounts of these ions by IR analyses.

In contrast to $Cr[M(CN)_6]$ (M = V, Cr, Mn), two broad ν_{CN} absorptions are observed at 2096 and 2143 cm^{-1} (Table 1) for M = Fe. The 2143 cm^{-1} absorption is consistent with $Cr-N\equiv C-Fe^{III}$ linkages, as stated above as well as previously reported $[Fe^{III}(CN)_6]^{3-}$-containing PBAs where $M^{II}-N\equiv C-Fe^{III}$ linkages are formed (M = Mn, Co, Ni, Cu, Zn, Cd) with the ν_{CN} absorption ranging from 2152 to 2187 cm^{-1}.[25] However, the 2096 cm^{-1} absorption is actually decreased from that of the parent cyanometalate ν_{CN} absorption and is more consistent with $Cr-N\equiv C-Fe^{II}$ linkages. $(NEt_4)_4[Fe^{II}(CN)_6]$ exhibits ν_{CN} absorptions at 2030(s), 2050(vs), and 2080(m) cm^{-1},[26] and upon bridging to another metal ion it shifts to higher energy with respect to these values.[24] Prussian blue itself, which contains $Fe^{III}-N\equiv C-Fe^{II}$ linkages, exhibits a broad absorption at 2080 cm^{-1}.[27] Iron existing in both the $[Fe^{II}(CN)_6]^{4-}$ and $[Fe^{III}(CN)_6]^{3-}$ forms has previously been reported for two different manganese hexacyanoferrates from which two ν_{CN} absorptions are observed for these binding motifs (i.e., $Mn-N\equiv C-Fe^{II}$ and $Mn-N\equiv C-Fe^{III}$).[28] Therefore, in this iron-containing compound, $(NEt_4)_{0.04}Cr_{1.04}[Fe(CN)_6](BF_4)_{0.16}\cdot 1.02MeCN$ (**4**), the Fe atom likely exists in both the Fe^{II} and Fe^{III} oxidation states. It should be noted that the Fe^{II}/Fe^{III} ratio cannot be exactly determined from the IR spectrum; therefore, $^{57}Fe-$Mössbauer spectroscopy was used to confirm the presence of both oxidation states as well as to obtain this ratio (vide infra). When Fe^{III} is reduced to Fe^{II}, the Cr^{III} atom must be oxidized to a higher oxidation state (i.e., Cr^{IV}) giving a mixed-valent material in both Fe and Cr.[29] In acid solutions, Cr^{IV} is a very strong oxidant ($E^0_{Cr^{IV}/Cr^{III}}$ of 2.1 V) and is unsurprisingly very reactive;[30] however, the oxidation of Cr^{III} complexes by hexacyanoferrate(III) to form Cr^{IV} species has been previously reported in alkaline solutions.[31] Cr^{IV} is likely stabilized after formation in the solid state. Compound **4** also shows the presence of small amounts of NEt_4^+, BF_4^-, as well as coordinated and noncoordinated MeCN. The samples chosen for other characterizations were verified to have minimal amounts of these species by IR analyses.

Thermal Stability. The thermal properties of $Cr[M(CN)_6]$ (M = V, Cr, Mn, Fe) were analyzed by TGA/MS. In general, each compound showed a rapid loss of MeCN and cyanide just above room temperature (~40 °C) followed by a continuous gradual mass loss up to 600 °C, all resulting in black residues. Due to this gradual mass loss, which was attributed to simultaneous solvent loss and decomposition, the temperatures at which these events occurred are indistinguishable. Nevertheless, the total mass losses were determined to be 46.5, 45.9, 39.3, and 52.1% for **1**, **2**, **3**, and **4**, respectively. TGA plots are provided as Supporting Information (Figure S2). Overall, these compounds are not very thermally stable due to their facile loss of MeCN and cyanide at relatively low temperatures (~40 °C); therefore, these compounds were stored and handled at −25 °C, and exposure to ambient temperatures was minimized. Drying of the samples before analyses was performed at room temperature under vacuum to avoid any thermal decomposition at elevated temperatures. The thermal instability observed for these compounds is a likely source of error in the elemental analyses. Due to the time required to obtain the elemental analyses off site, thermal decomposition may have occurred, contributing to larger than desired errors in the elemental percentages.

Powder X-ray Diffraction. PBAs adopt a fcc structure with a lattice constant (*a*) ranging from 9.9 to 10.9 Å.[1,4,7] The diffraction patterns of **1**−**4** have weak, broad peaks indicative of being completely amorphous, and none of the patterns could be indexed to the fcc structure (Figure S4, Supporting Information). In the previous $Cr^{III}[Mn^{III}(CN)_6]$ PBA, reported by Buschmann et al.,[15] a small fraction of the material was determined to be crystalline and this fraction was indexed to the fcc PBA structure with a lattice constant *a* of 9.5 Å. Overall, these compounds are amorphous and hence structurally disordered. This results in small sample-to-sample variations in both the structural and magnetic properties. The synthesis of more crystalline samples was attempted by varying the addition rate in the reaction conditions; however, all samples were concluded to be amorphous regardless of synthetic procedure.

^{57}Fe−Mössbauer Spectroscopy. ^{57}Fe−Mössbauer spectra for **4** were recorded at 1.4, 4.2, 48, and 298 K (Figure 1 and Table 2). The 48 K data demonstrates that the Fe ions exist as valence-trapped Fe^{II} and Fe^{III}, consistent with the two ν_{CN}

(25) Martínez-Garcia, R.; Knobel, M.; Reguera, E. *J. Phys. Chem. B* **2006**, *110*, 7296.
(26) Eller, S.; Fischer, R. D. *Inorg. Chem.* **1990**, *29*, 1289.
(27) Ghosh, S. N. *J. Inorg. Nucl. Chem.* **1974**, *36*, 2465.
(28) (a) Vertelmann, E. J. M.; Maccallini, E.; Gournis, D.; Rudolf, P.; Bakas, T.; Luzon, J.; Broer, R.; Pugzlys, A.; Lummen, T. T. A.; van Loosdrecht, P. H. M.; van Koningsbruggen, P. J. *Chem. Mater.* **2006**, *18*, 1951. (b) Matsuda, T.; Tokoro, H.; Hashimoto, K.; Ohkoshi, S. *Dalton Trans.* **2006**, 5046.
(29) Alternatively, if Cr was reduced to Cr^{II} and Fe was oxidized to Fe^{IV}. In this situation, the n_{CN} absorption would likely be above 2150 cm^{-1} for a $Cr-N\equiv C-Fe^{IV}$ linkage, and this is not observed. However, if a linkage isomerism of the cyanide occurred, then Cr^{II} would be carbon-bound to cyanide and the 2096 cm^{-1} value would be consistent. These oxidation states do not fit the magnetic data and are therefore considered less likely.
(30) Shriver, D. F.; Atkins, P. W. *Inorganic Chemistry*, 3rd ed.; Oxford University Press, 1999.
(31) Katafias, A.; Impert, O.; Kita, P.; Wrzeszcz, G. *Trans. Met. Chem.* **2004**, *29*, 855. Chatlas, J.; Impert, O.; Katafias, A.; Kita, P.; Wrzeszcz, G.; Eriksen, J.; Monsted, O.; Mills, A. *Trans. Met. Chem.* **2004**, *29*, 634. Tuwar, S. M.; Nandibewoor, S. T.; Raju, J. R. *Trans. Met. Chem.* **1991**, *16*, 335.

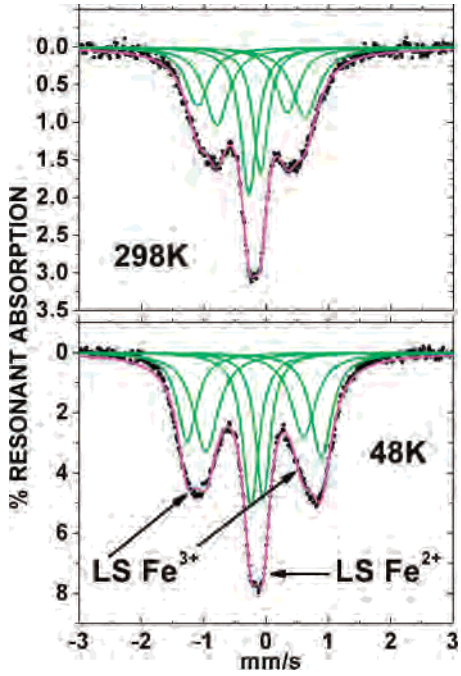

Figure 1. ^{57}Fe−Mössbauer spectra of **4** at 298 K (top) and 48 K (bottom) vs iron metal. Lorentzian fits are shown in solid lines for the quadrupole doublets (1,6), (2,5), and (3,4).

Table 2. ^{57}Fe−Mössbauer Parameters for **4** at 48 and 298 K Relative to Fe for Quadrupole Doublets (1,6), (2,5), and (3,4)

Fe oxidation state	δ (mm/s), @ 48 K	ΔE (mm/s), @ 48 K	δ (mm/s), @ 298 K	ΔE (mm/s), @ 298 K
II (transitions 3,4)	−0.073	0.19	−0.18	0.20
III (transitions 1,6	−0.19	2.15	−0.21	1.73
and 2,5)		1.57		1.13

absorptions observed in the IR data (vide supra). The Fe ions are in octahedral environments with carbon-bound cyanides linked to Fe, resulting in both Fe^{II} and Fe^{III} being low spin. There are at least two inequivalent low-spin Fe^{III} sites, as suggested by the observation of two such doublets (1,6) and (2,5) (Table 2 and Figure 1). The origin of this behavior is not clear at this time. The isomer shifts (δ) for Fe^{II} and Fe^{III} are −0.073 and −0.19 mm/s, respectively. These isomer shifts are similar to those reported previously for $[Fe^{II}(CN)_6]^{4-}$ and $[Fe^{III}(CN)_6]^{3-}$ [28a,32] and consistent with low-spin d^6 and d^5. Fe^{II} is diamagnetic with a $t_{2g}^6e_g^0$ electron configuration. The corresponding $^1A_{1g}$ ground term usually has little or no valence-shell-electron contribution to the electric field gradient tensor and therefore exhibits a small or near zero quadrupole splitting. In contrast, Fe^{III} has a $t_{2g}^5e_g^0$ electron configuration for which a significant, temperature-dependent quadrupole splitting effect is possible and observed herein. Lorentzian fits of the data lead to an Fe^{II}/Fe^{III} ratio of ∼0.4:0.6 at 48 and 298 K. With the use of this ratio, elemental analysis, and taking into consideration charge neutrality, **4** was formulated to be $(NEt_4)_{0.04}Cr^{III}_{0.6}Cr^{IV}_{0.4}[Fe^{II}(CN)_6]_{0.4}[Fe^{III}(CN)_6]_{0.62}(BF_4)_{0.16}\cdot 1.02MeCN$.

At 4.2 K, the outer low-spin ferric resonances of **4** are broadened while, as expected, nothing happens to the intensity or line width of the central singlet corresponding to diamagnetic low-spin Fe^{II}. Below 3 K, the intensity associated with the Fe(III) sites completely disappears, consistent with a transformation from the rapidly relaxing paramagnetic form of **4** to an ordered state, as suggested by magnetization data (vide infra). Nevertheless, a resolved magnetic hyperfine pattern (a typical nuclear Zeeman splitting sextet) is not observed at our limiting low temperature (∼1.4 K), indicating that critical fluctuations are still important on the Mössbauer spectroscopy time scale at these temperatures.

Table 3. Summary of Magnetic Properties for $(NEt_4)_3[M^{III}(CN)_6]$ (M = V, Cr, Mn, Fe)

M^{III}	S	χT_{obs} (at RT) (emu·K/mol)	g	θ (K)
V	1	0.78	1.82	−26
Cr	$^3/_2$	1.89	2.00	−1.5
Mn	1	1.52	2.48	−3.8
Fe	$^1/_2$	0.54	2.64	−60

Magnetic Susceptibility. Before discussing the magnetic properties of compounds **1**−**4**, the temperature dependencies of the magnetic susceptibilities, $\chi(T)$, for the parent cyanometalates, $(NEt_4)_3[M^{III}(CN)_6]$ (M = V, Cr, Mn, Fe), were studied.

$(NEt_4)_3[M^{III}(CN)_6]$ (M = V, Cr, Mn, Fe). $\chi(T)$ values of $(NEt_4)_3[M^{III}(CN)_6]$ (M = V, Cr, Mn, Fe) were measured between 5 and 300 K. Above 50 K (M = V, Cr) and above 100 K (M = Mn, Fe), the data for these parent cyanometalates were fit to the Curie−Weiss expression, $\chi \propto (T-\theta)^{-1}$, with θ values ranging from −1.5 (M = Cr^{III}) to −60 K (M = Fe^{III}) and the Landé g values ranging between 1.82 (M = V^{III}) and 2.64 (M = Fe^{III}) (Table 3 and Figure S3). The g value of 1.82 for $(NEt_4)_3[V^{III}(CN)_6]$ is in good agreement with g = 1.88 reported for $K_3[V^{III}(NCS)_6]\cdot 4H_2O$.[16,33] Values of g for $(NEt_4)_3[Cr^{III}(CN)_6]$ (g = 2.00), $(NEt_4)_3[Mn^{III}(CN)_6]$ (g = 2.48), and $(NEt_4)_3[Fe^{III}(CN)_6]$ (g = 2.64) are all consistent with literature values reported previously (for $K_3[Cr^{III}(CN)_6]$ g = 2.00,[34] for $K_3[Mn^{III}(CN)_6]$ g = 2.47,[35] and for $K_3[Fe^{III}(CN)_6]$ g = 2.60[36]). The large g values observed for Mn and Fe hexacyanometalates are attributed to large magnetic anisotropy arising from appreciable orbital contribution.[37] Room-temperature χT values range between 0.54 (M = Fe) and 1.89 (M = Cr) emu·K/mol (Table 3), and from the $\chi T(T)$ data it is clear that these cyanometalates, in an octahedral environment, are low spin, as expected for the strong field cyanide ligand.

(32) (a) Greenwood, N. N.; Gibb, T. C. In *Mössbauer Spectroscopy*; Chapman and Hall, Ltd.: London, 1971; pp 169−182. (b) Sato, O.; Einaga, Y.; Fujishima, A.; Hashimoto, K. *Inorg. Chem.* **1999**, *38*, 4405.

(33) Boudreaux, E. A.; Mulay, L. N. In *Theory and Applications of Molecular Paramagnetism*; Wiley-Interscience: New York, 1976; p 159. Figgis, B. N.; Lewis, J.; Mabbs, F. *J. Chem. Soc.* **1960**, 2480.

(34) Baker, J. M.; Bleaney, B.; Bowers, K. D. *Proc. Phys. Soc.* **1956**, *B 69*, 1205.

(35) Cooke, A. H.; Duffus, H. J. *Proc. Phys. Soc.* **1955**, *A 68*, 32. Kamimura, H. *J. Phys. Soc. Jpn.* **1956**, *11*, 1171. Udachin, Y. N. Dyatkina, M. E. *J. Struct. Chem.* **1967**, *8*, 325.

(36) Figgis, B. N.; Gerloch, M.; Mason, R. *Proc. Roy. Soc. London* **1969**, *A 309*, 91.

(37) Sharpe, A. G. In *The Chemistry of Cyano Complexes of the Transition Metals*; Academic Press: New York, 1976.

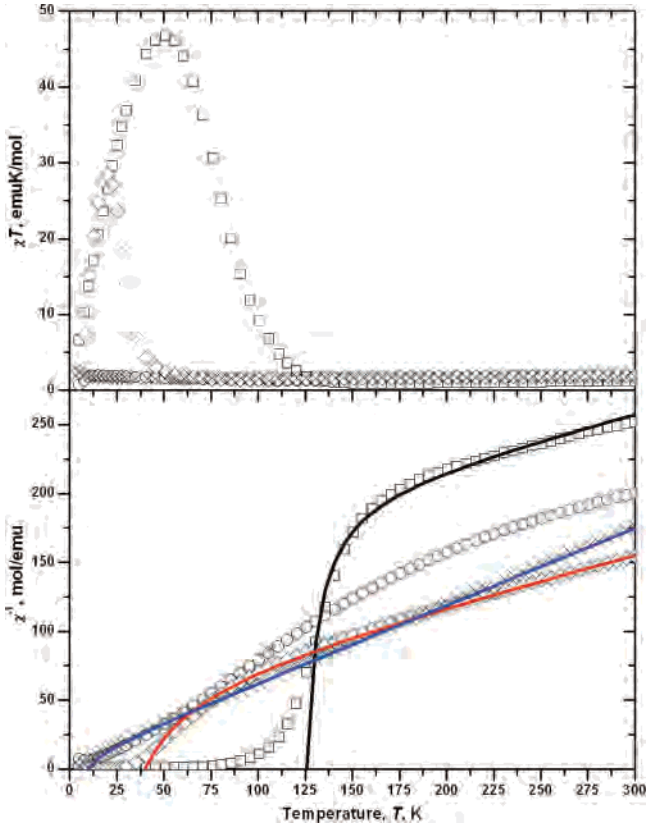

Figure 2. $\chi T(T)$ (top) and $\chi^{-1}(T)$ (bottom) for **1** (○), **2** (□), **3** (◇), and **4** (×). Fits to Néel's hyperbolic equation, eq 6, for **2**−**4** are displayed with solid lines (**2** (black), **3** (red), and **4** (blue)). Samples were cooled in a zero applied field to 5 K, and data was measured upon warming in a 500 Oe applied field.

Table 4. Summary of Magnetic Properties for **1**−**4**

	1	**2**	**3**	**4**
χT_{obs}, emu·K/mol (room temperature)	1.50	1.91	2.12	1.70
χT_{calc}, emu·K/mol (spin only)	2.69	3.75	3.41	1.99
$\chi T(T-\theta)_{calc}$, emu·K/mol	1.57	1.37	2.37	1.92
θ, K (Curie−Weiss)	−212	−524	−132	−12
θ, K (Néel)	[a]	−465	−162	−12
T_N, K (dc)	[a]	126	40	10
T_{onset}, K (ZFC)	21	82	28	6
T_b, K (ZFC/FC)	10	110	20	5
T_c, K (ac)	11	100	24	3
T_f, K (ac)	10	30	19	2.5
ϕ (ac)	0.020	0.022	0.032	0.040
H_{cr}, Oe	790	35	375	17
M, emu·Oe/mol, (at 90 kOe)	2670	1480	5260	10510
M_{rem}, emu·Oe/mol	110	200	430	10

[a] Unable to be fit to Neél's hyperbolic equation (eq 6).

Cr[M(CN)$_6$] (M = V, Cr, Mn, Fe). The $\chi(T)$ values of **1**−**4** were measured between 2 and 300 K. The data above 225 K for **1**, 250 K for **2**, 150 K for **3**, and 50 K for **4** were fit to the Curie−Weiss expression, $\chi \propto (T-\theta)^{-1}$, with θ values of −12 K (M = Fe) to −132 (for M = Mn), −212 (for M = V), and −524 K (M = Cr) (Table 4 and Figure 2). All of these compounds exhibit antiferromagnetic coupling from the negative θ values with strong coupling being observed for M = V, Cr, Mn and weak coupling being observed for M = Fe. The weak coupling in the iron-containing compound is due to the presence of diamagnetic $[Fe^{II}(CN)_6]^{4-}$. The observed antiferromagnetic coupling is in accord with the interactions of spins in nonorthogonal orbitals (i.e., unpaired spins interacting between $t_{2g}-t_{2g}$ orbitals). The spin states of the hexacyanometalate(III) ions in these PBAs are identical to the parent cyanometalate compounds, which are summarized in Table 3. In **4**, as a result of a partial electron transfer between Cr^{III} and Fe^{III} along the $Cr^{III}-NC-Fe^{III}$ linkages, the formation of $Cr^{IV}-N\equiv C-Fe^{II}$ results in the presence of diamagnetic ($S = 0$) $[Fe^{II}(CN)_6]^{4-}$ ions and $S = 1$ Cr^{IV} ions (g value for Cr^{IV} was taken to be 2.00[38]). The nitrogen-bound Cr^{III} atoms in the Cr[M(CN)$_6$] (M = V, Cr, Mn, Fe) family have a spin state of $S = {}^3/_2$ ($g = 2.00$).[17] The spin and g values for these cyanometalates, the nitrogen-bound Cr ion, and the θ values for the Cr[M(CN)$_6$] compounds were used to determine the calculated $\chi T(T-\theta)$ values reported in Table 4, which are in good agreement with the observed values.

In addition to the $\chi(T)$ measurements at 500 Oe, magnetic ordering was confirmed in these samples by performing several other magnetic analyses, including low-field magnetization (zero field cooled [$M_{ZFC}(T)$]/field cooled [$M_{FC}(T)$]) (Figure 3), ac-susceptibility (χ_{ac}) measurements (Figure 4), and field-dependence of magnetizations [$M(H)$] (Figures 5 and 6). These results are qualitatively reproducible but have some variance in the transition temperatures and absolute magnetization values due to the disorder and thermal instability discussed above. The key magnetic results (i.e., T_c, H_{cr}, etc.) are summarized in Table 4, and the magnetic properties of **1**−**4** are discussed below.

Compound 1. Compound **1** has a room-temperature χT value of 1.50 emu·K/mol that is substantially lower than the spin-only value of 2.69 emu·K/mol (for Cr^{III}, $S = {}^3/_2$ and $g = 2$; and for V^{III}, $S = 1$ and $g = 1.82$). Above 225 K, $\chi(T)$ was fit to the Curie−Weiss expression with $\theta = -212$ K indicating that strong antiferromagnetic coupling dominates the short-range exchange. Similar, large negative θ values are observed for other hexacyanovanadate-based PBAs, and these values range from −150 to −445 K.[16,39] With the use of this θ value, the $\chi T(T-\theta)_{calc}$ value is found as 1.57 emu·K/mol, in good agreement with the observed value and the formulation of $(NEt_4)_{0.02}Cr^{III}[V^{III}(CN)_6]_{0.98}(BF_4)_{0.08}\cdot 0.10MeCN$ established from the IR and the observed elemental composition. As the temperature is lowered, the $\chi T(T)$ value gradually decreases to a minimum of 1.22 emu·K/mol at 140 K, then begins to increase more gradually to a maximum of 1.90 emu·K/mol at 15 K, before decreasing rapidly below 15 K to 0.69 emu·K/mol at 5 K (Figure 2). This rise in $\chi T(T)$ to a maximum is consistent with a magnetically ordered system; however, the onset of magnetic ordering is unclear from the $\chi T(T)$ data due to the gradual increase of the data with decreasing temperature. As a consequence, the exact ordering temperature was determined via alternate methods (vide

(38) Boudreaux, E. A.; Mulay, L. N. In *Theory and Applications of Molecular Paramagnetism*; Wiley-Interscience: New York, 1976; p 161. Ba_2CrO_4 and Sr_2CrO_4 both obey the Curie law with a g value of 2.04; in addition, K_2CrF_6 has a g value of 1.98.
(39) Entley, W. R.; Girolami, G. S. *Science* **1995**, *268*, 397.

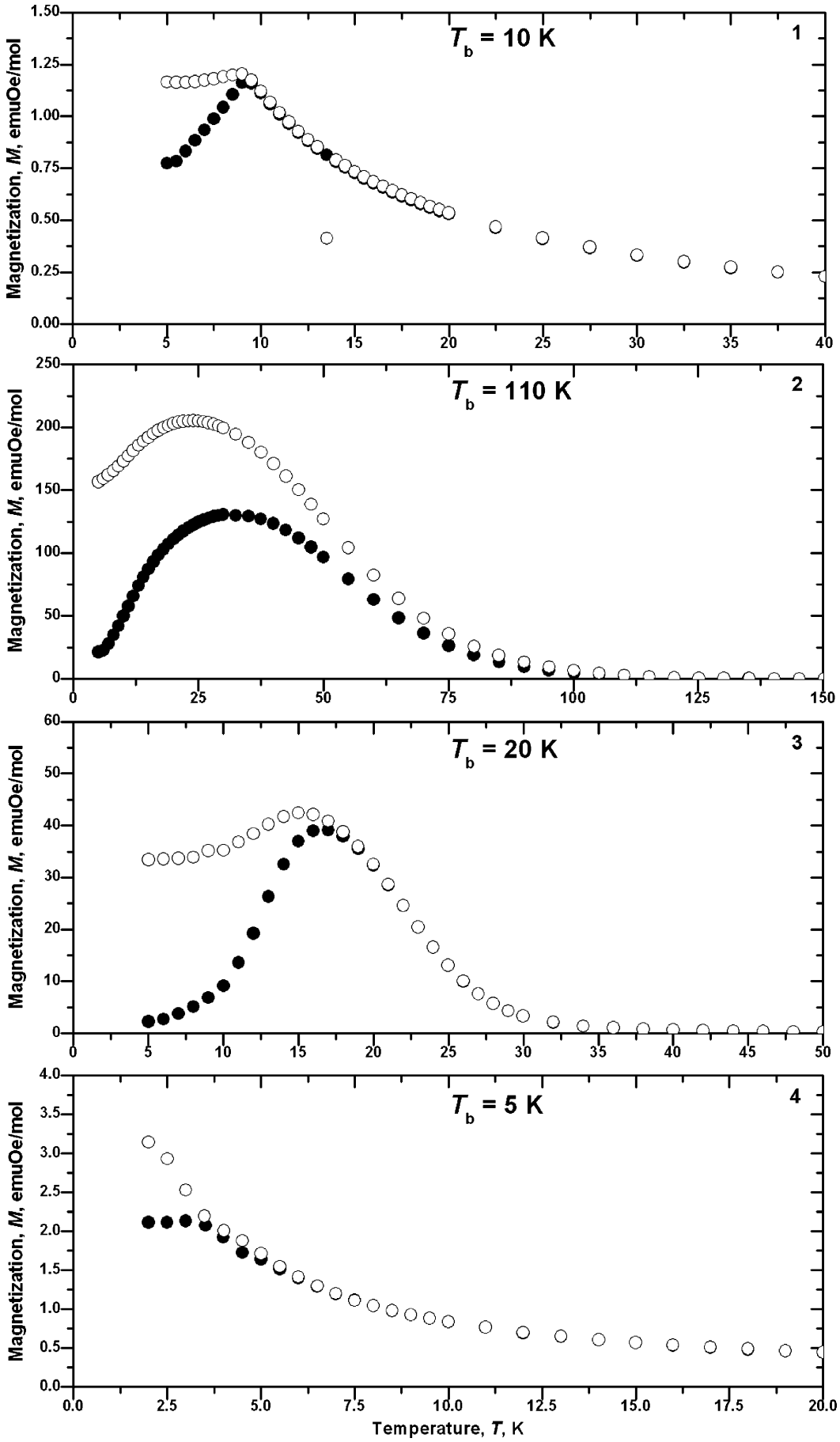

Figure 3. 5 Oe M_{ZFC} (●) and M_{FC} (○) $M(T)$ data for **1**−**4**.

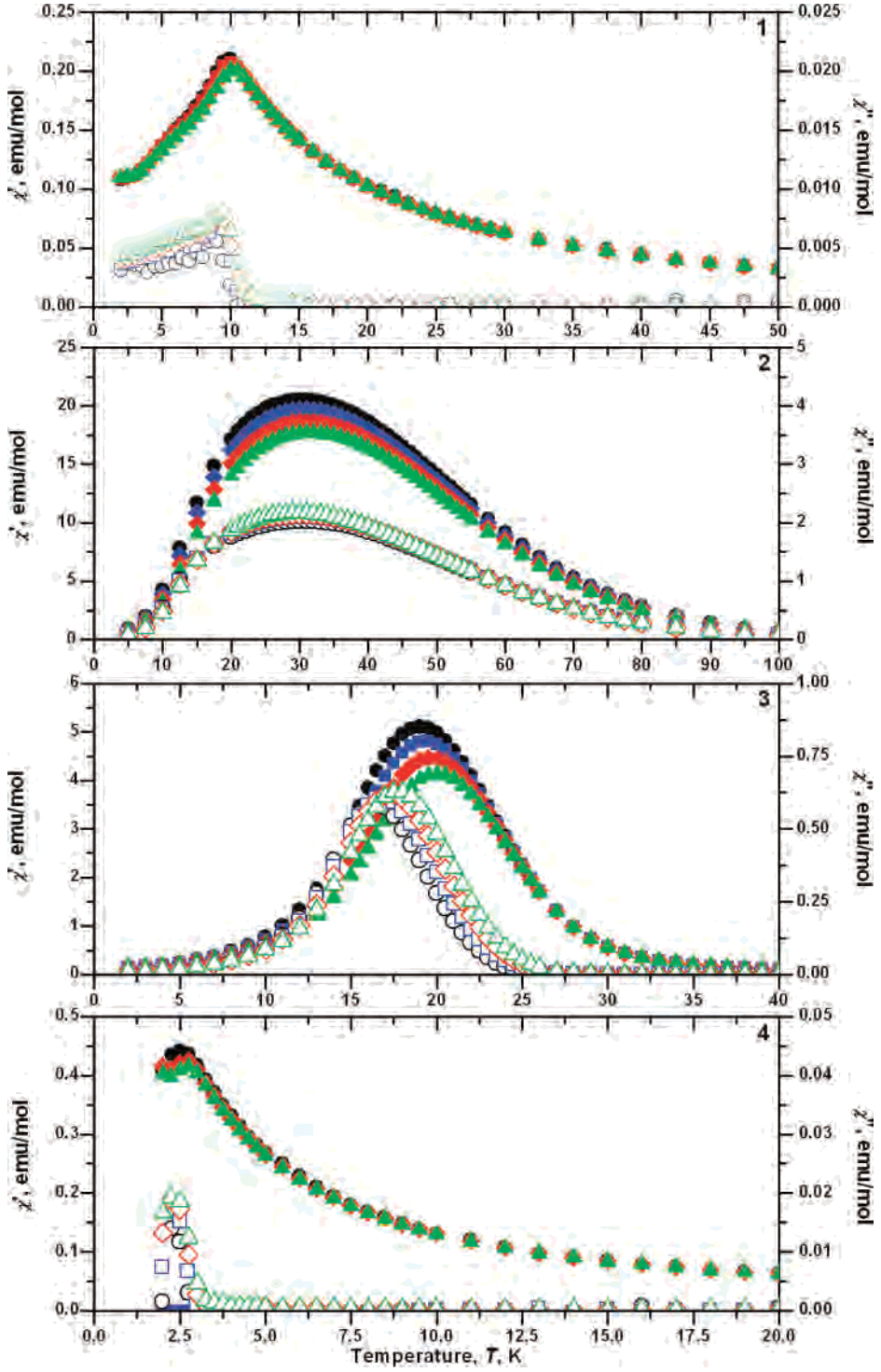

Figure 4. Observed in-phase, $\chi'(T)$ (closed symbols) and out-of-phase, $\chi''(T)$ (open symbols), ac responses for **1**, **2**, **3**, and **4** at 33 (○), 100 (□), 333 (◇), and 1000 Hz (Δ) at zero applied field.

infra). Nevertheless, the minimum in $\chi T(T)$ observed at 140 K (above the expected ordering temperature) is consistent with a ferrimagnet and is a consequence of short-range antiferromagnetic correlations resulting in a cancellation of spins.[40,41] **1** is therefore a ferrimagnet where the Cr^{III} spins, $S = {}^3/_2$ ($t_{2g}{}^3$), and the V^{III} spins, $S = 1$ ($t_{2g}{}^2$), are antiferromagnetically coupled. Attempts to fit the $\chi^{-1}(T)$ function to the hyperbolic equation, eq 6, based on Néel's theory[41]

$$\chi^{-1} = \frac{T-\theta}{C} - \frac{\zeta}{T-\theta'} \qquad (6)$$

(where C and θ are the Curie and Weiss constants, respectively, and θ' and ζ are proportional to $\eta_A\eta_B C(\eta_A - \eta_B)$ and $\eta_A\eta_B C$ (where η_i is the fractional occupancy of each

(40) (a) Stumpf, H. O.; Pei, Y.; Kahn, O.; Sletten, J.; Renard, J. P. *J. Am. Chem. Soc.* **1993**, *115*, 6738. (b) Stumpf, H. O.; Ouahab, L.; Pei, Y.; Bergerat, P.; Kahn, O. *J. Am. Chem. Soc.* **1994**, *116*, 3866.

(41) (a) Néel, L. *Ann. Phys.* **1948**, *3*, 137. (b) Smart, J. S. *Am. J. Phys.* **1955**, *23*, 356.

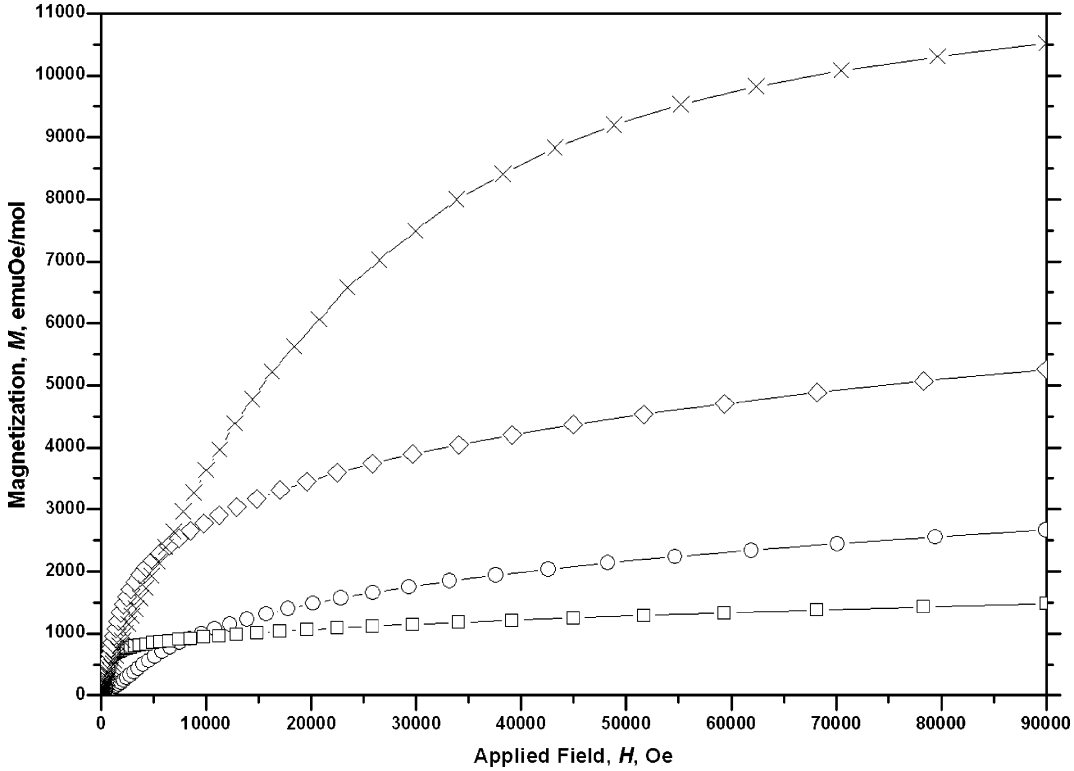

Figure 5. $M(H)$ data for **1** (○), **2** (□), **3** (◇), and **4** (×) up to 90 kOe.

sublattice site), respectively) and ultimately obtain the Néel temperature, T_N, were unsuccessful. The inability to fit the data to Néel's hyperbolic equation is due to the gradual increase and low magnitude in the peak of the $\chi T(T)$ data. This is likely due to this compound having small ferrimagnetic spin domains that are separated by a larger sea of paramagnetic spins resulting in the ferrimagnetic domains with weak interactions throughout the bulk material. This is a cluster-glass behavior, and at sufficiently low temperature, these ferrimagnetic clusters will freeze in a random orientation similar to spin-glass materials.[42] Ac-susceptibility measurements will help to confirm this hypothesis (vide infra).

Low-field $M(T)$ measurements are used to determine key information about an ordering system, and low-field $M_{ZFC}(T)/M_{FC}(T)$ of **1** shows the onset of magnetic ordering, T_{onset}, below 21 K (by extrapolation of the steepest slope to the T where $M = 0$) and a blocking temperature, T_b, is at 10 K (Figure 3). This blocking temperature is the temperature where the $M_{ZFC}(T)/M_{FC}(T)$ data converge, and below this temperature there is a certain irreversibility (or hysteresis) in these magnetizations as a result of the material entering the magnetically ordered state. The decrease in magnetization below the peak in the $M_{ZFC}(T)/M_{FC}(T)$ data is consistent with this sample having strong antiferromagnetic interactions resulting in ferrimagnetic behavior. Again, the low magnetization of the sample at low fields suggests that bulk material has small ferrimagnetic domains that are well-separated by paramagnetic regions overall, resulting in a low response in $M(T)$.

The frequency-dependent in-phase, $\chi'(T)$, and out-of-phase, $\chi''(T)$, components of the ac susceptibility can also be used to determine the magnetic ordering temperatures. In a zero applied dc field, **1** exhibits a response in both $\chi'(T)$ and $\chi''(T)$ with a magnetic ordering temperature of 11 K (from the initial rise in the $\chi''(T)$ data upon cooling) (Figure 4). This ordering temperature is consistent with the blocking temperature obtained in the $M_{ZFC}(T)/M_{FC}(T)$ data. **1** has an observable frequency dependence, $\phi = 0.020$, which is attributed to a spin- or cluster-glass behavior.[42] Spin- or cluster-glass behavior has been reported for other PBAs and is indicative of a more disordered and/or amorphous material.[16,43] This is consistent with the PXRD data where this compound is amorphous and structurally disordered (vide supra). The temperature at which the maximum in the $\chi'(T)$ data becomes frequency dependent corresponds to the temperature at which the magnetic moments of this disordered material become frozen, and this is termed the freezing temperature, T_f. T_f for **1** is determined (by peak in the $\chi'(T)$ at 33 Hz) to be 10 K. The spin- or cluster-glass behavior supports the hypothesis that there are small ferrimagnetic domains separated by a sea of paramagnetic spins. At T_f (10 K), the spins in these ferrimagnetic domains are randomly

(42) Mydosh, J. A. In *Spin Glasses: An Experimental Introduction*; Taylor and Francis: London, 1993; p 67. ϕ is a parameter indicative of the amount of spin disorder in a material known as spin-glass behavior: $\phi = \Delta T_{max}/[T_{max}(\Delta \log \omega)]$, where ΔT_{max} = difference between peak maximum of the temperatures at the high and low frequencies, T_{max} = peak maximum of the temperature at low frequency, and $\Delta \log \omega$ = difference in the logarithms of the high and low frequencies (ω).

(43) (a) Buschmann, W. E.; Ensling, J.; Gütlich, P.; Miller, J. S. *Chem.—Eur. J.* **1999**, *5*, 3019. (b) Sendek, M.; Csach, K.; Kavecansky, V.; Lukácová, M.; Marysko, M.; Mitróová, Z.; Zentko, A. *Phys. Status Solidi A* **2003**, *196*, 225.

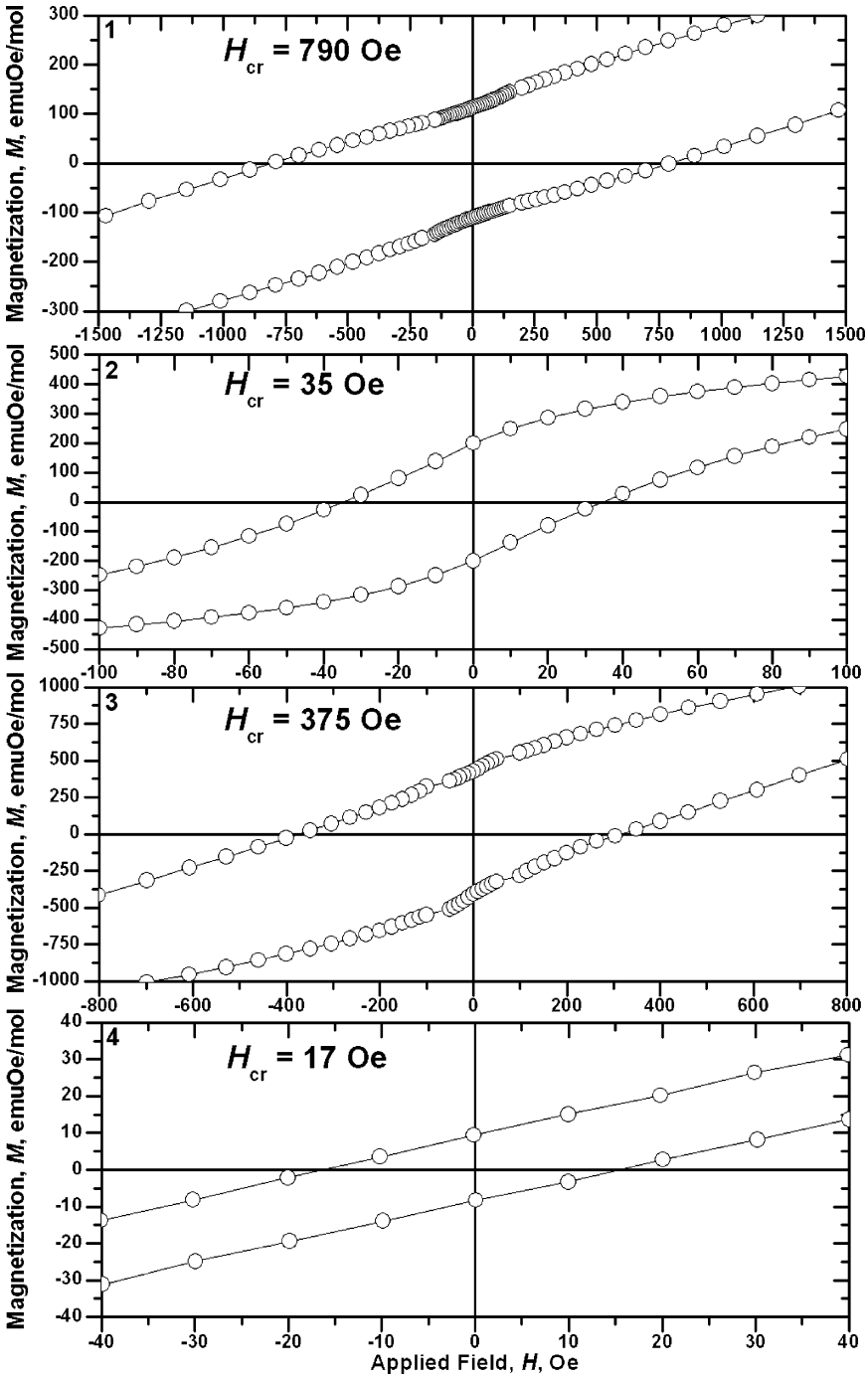

Figure 6. $M(H)$ hysteresis curves for **1**−**4** showing the changes in H_{cr}.

frozen and result in an overall net moment, causing an increase in the $\chi(T)$ values and a response in the $\chi_{ac}(T)$ values.

$M(H)$ measurements at 2 K show that **1** is far from saturation even at 90 kOe where a magnetization value of 2670 emu·Oe/mol is observed (Figure 5). At low temperature, the spins in this system (for Cr^{III}, $S = {}^3/_2$ and $g = 2$; and for V^{III}, $S = 1$ and $g = 1.82$) should be antiferromagnetically aligned, resulting in an expected saturation magnetization value of 6587 emu·Oe/mol. Hysteresis was also observed for **1** at 2 K (coercive field, H_{cr}, of 790 Oe) with a remanent magnetization, M_{rem}, of 110 emu·Oe/mol (Figure 6). The large coercive field is attributed to the glassy behavior discussed above.

The data above are consistent with **1** being a spin- or cluster-glass material with a T_f value of 10 K. Below this temperature, small ferrimagnetic domains are frozen randomly, resulting in an overall bulk response of magnetic ordering. This glassy behavior is caused by the material being amorphous and structurally disordered, and has been demonstrated for PBAs in the literature before.[16] With this compound being the first hexacyanovanadate(III)-based PBA, few comparisons can be made; however, on comparing the magnetic properties of **1** to the high-T_c vanadium hexacyanochromate(III) magnets,[7,8] it is clear that the magnetic ordering is drastically reduced by changing the cyanides binding motif (i.e., linkage isomerism of the cyanide ligand).

The coupling is still strongly antiferromagnetic ($\theta = -212$ K), but the significant glassy behavior results in a poor communication of this strong coupling throughout the bulk material, ultimately leading to a low-T_c material.

Compound 2. Compound **2** has a room-temperature χT value of 1.19 emu·K/mol that is again substantially lower than the spin-only value of 3.75 emu·K/mol (for Cr^{III}, $S = 3/2$ and $g = 2$). Above 250 K, $\chi(T)$ was fit to the Curie−Weiss expression with $\theta = -524$ K, indicating that very strong antiferromagnetic coupling dominates the short-range exchange. With the use of this θ value, the $\chi T(T - \theta)_{calc}$ value is 1.37 emu·K/mol, which is more consistent with the observed room-temperature χT value. As the temperature is lowered, the $\chi T(T)$ value gradually decreases to a minimum of 0.85 emu·K/mol at 140 K before $\chi T(T)$ begins to increase rapidly to a maximum of 46.7 emu·K/mol at 51 K, indicative of magnetic ordering. As the temperature is lowered further, $\chi T(T)$ decreases rapidly to 6.57 emu·K/mol at 5 K (Figure 2). Again, a minimum in the $\chi T(T)$ value is observed above the ordering temperature that is characteristic of ferrimagnets.[40,41] In **2**, the spins on the Cr^{III} atom are $S = {}^3/_2$ ($t_{2g}{}^3$) and $g = 2$ in both ligand environments ($Cr^{III}-N\equiv C-Cr^{III}$); therefore, the spins should be completely compensated, resulting in a perfect antiferromagnet. However, as seen in the $\chi T(T)$ data, this is not observed and is attributed to some of the spins being canted, resulting in a noncompensation of the spins. Canting is likely due to the amorphous and structurally disordered nature of this material. Nevertheless, this canted antiferromagnet behaves similarly to a ferrimagnet. Above 125 K, $\chi^{-1}(T)$ for **2** can be fit to eq 6[41] with a T_N value of 126 K. A θ value of −465 K was also obtained from this fit and confirms the observed strong antiferromagnetic coupling in the high-temperature region. Strong antiferromagnetic coupling has been observed in other chromium hexacyanochromate(III) PBAs (θ values ranging from −119 to −440 K),[5,6,14a] and in **2** the antiferromagnetic interactions are the highest.

Low-field $M_{ZFC}(T)/M_{FC}(T)$ of **2** show the onset of magnetic ordering, T_{onset}, below 82 K and a blocking temperature, T_b, of 110 K (Figure 3). In this sample the blocking (irreversibility) temperature of 110 K is significantly higher than the onset of magnetization. Explanations for this phenomenon could be the presence of spin domains and/or multiple magnetic phases in the bulk material. Though complex in its nature, it is clear that **2** enters a magnetically ordered state at ∼110 K, which is caused by canting of the spins in this sample that should be a perfect antiferromagnet. Similar to **1**, in the $M_{ZFC}(T)/M_{FC}(T)$ data for **2**, there is a decrease in magnetization below the peak that confirms antiferromagnetic interactions leading to ferrimagnetic behavior.

In a zero applied dc field, **2** exhibits broad peaks in both a $\chi'(T)$ and $\chi''(T)$ responses with a magnetic ordering temperature of 100 K (Figure 4). This ordering temperature is consistent with blocking temperature obtained in the $M_{ZFC}(T)/M_{FC}(T)$ data. The broadness of the peaks in both the $\chi'(T)$ and $\chi''(T)$ data can be explained by **2** having several magnetic phases in the bulk material. The portion of the bulk material that orders at 100 K is smaller than the portion(s) that orders between 25 and 60 K. Nevertheless, it is clear that at 100 K the sample does begin to magnetically order. **2** has an observable frequency dependence in the $\chi_{ac}(T)$ data, $\phi = 0.022$, that is attributed to a spin- or cluster-glass behavior.[42] Again, this behavior has been reported for PBAs before and indicates a disordered and/or amorphous material,[16,43] which was confirmed by PXRD studies. The freezing temperature, T_f, of **2** is 30 K; however, this is an average freezing temperature. This spin- or cluster-glass behavior could be the source of the spins canting, giving this antiferromagnet its' ferrimagnetic behavior. From the data above, it is concluded that **2** is a canted antiferromagnet with a cluster-glass-like behavior, which has several different spin domains resulting in complex magnetic properties.

The 2 K $M(H)$ data show that **2** does not saturate at 90 kOe where a magnetization value of 1480 emu·Oe/mol is observed (Figure 5). This observed value of 1480 emu·Oe/mol is consistent with canting of the spins, which again is caused by the structural disorder associated with the sample being amorphous. Hysteresis was also observed for **2** at 2 K (H_{cr} of 35 Oe) with a M_{rem} value of 200 emu·Oe/mol (Figure 6).

The above data is consistent with **2** being a spin- or cluster-glass material with $T_f = 30$ K; however, bulk magnetic response is observed at a higher critical temperature, T_c, of 100 K (ac data) arising from the strong antiferromagnetic interactions ($\theta = -524$ K). This phenomenon can be explained by the sample having several magnetic phases that order at different temperatures with the highest being 100 K. These magnetic phases and glassy behavior are a consequence of **2** being amorphous and structurally disordered. The T_c value for **2** is the highest in this family of PBAs, $Cr[M(CN)_6]$ (M = V, Cr, Mn, Fe); however, it is substantially lower than the chromium(III) hexacyanochromate(III) PBA prepared electrochemically ($T_c = 230$ K)[6] and other chromium hexacyanochromate(III) PBAs reported in the literature with T_c's ranging from 150 K to the highest at 270 K.[5,6,14]

Compound 3. Compound **3** has a room-temperature χT value of 2.12 emu·K/mol that is substantially lower than the spin-only value of 3.41 emu·K/mol (Cr^{III}, $S = {}^3/_2$ and $g = 2$; and for Mn^{III}, $S = 1$ and $g = 2.48$). Above 150 K, $\chi(T)$ was fit to the Curie−Weiss expression with $\theta = -132$ K indicating that strong antiferromagnetic coupling dominates the short-range exchange. With the use of this θ value, the $\chi T(T - \theta)_{calc}$ value is 2.37 emu·K/mol, which is more consistent with that observed for the χT value at room-temperature. As the temperature is lowered, the $\chi T(T)$ value gradually decreases to a minimum of 1.49 emu·K/mol at 96 K and increases around 50 K reaching a maximum of 28.5 emu·K/mol at 20 K. This is indicative of magnetic ordering. Finally, the $\chi T(T)$ value decreases rapidly to 2.42 emu·K/mol at 5 K (Figure 2). The minimum in $\chi T(T)$ above the ordering temperature is characteristic of a ferrimagnet and as stated above is a consequence of the short-range antiferromagnetic correlations causing a cancellation of spins.[40,41] Above 125 K, $\chi^{-1}(T)$ was fit to eq 6 with a T_N value of 40

K. A θ value of -162 K was obtained from this fit and confirms strong antiferromagnetic coupling in the high-temperature region and falls within the range of -105 to -370 K observed for other hexcyanomanganese(III)-based PBAs.[15,44]

Low-field $M_{ZFC}(T)/M_{FC}(T)$ for **3** shows the onset of magnetic ordering, T_{onset}, below 28 K and a blocking (irreversibility) temperature, T_b, of 20 K (Figure 3). The decrease in magnetization below the peak in the $M_{ZFC}(T)/M_{FC}(T)$ data is a consequence of this sample having strong antiferromagnetic interactions, which ultimately result in a ferrimagnet. In the previous synthesis of this PBA $Cr^{III}[Mn^{III}(CN)_6]$, performed by Buschmann et al., the onset of magnetic ordering was determined to be 22 K (by extrapolation of the steepest slope to $M = 0$ in the $M_{ZFC}(T)/M_{FC}(T)$ data);[15] however, the blocking temperature of their material was not reported. Nevertheless, the onset of magnetic ordering was slightly enhanced from 22 K in Buschmann's compound to 28 K in **3** (27% increase). The reason for this difference is likely due to the different synthetic approaches of the two samples and will be discussed in more detail below.

The ac data reveals magnetic ordering from a response in both the $\chi'(T)$ and $\chi''(T)$ values, and a T_c value of 24 K was obtained (Figure 4). This critical temperature is somewhat consistent with the blocking temperature obtained in the $M_{ZFC}(T)/M_{FC}(T)$ data, below which this material enters a magnetically ordered state. Compound **3** has the second largest frequency dependence of this $Cr[M(CN)_6]$ series with $\phi = 0.032$. This ϕ value is consistent with spin- or cluster-glass behavior,[42] and as stated above, this glassy behavior has been reported for other PBAs and can attributed to the sample being a disordered and/or amorphous material.[16,43] Structural disorder was confirmed by PXRD of **3** where the sample was concluded to be completely amorphous (vide supra). The freezing temperature, T_f, of **3** is 19 K, which is consistent with the blocking temperature from the $M_{ZFC}(T)/M_{FC}(T)$ data. In the sample previously reported by Buschmann et al., $Cr^{III}[Mn^{III}(CN)_6]$, the rise in $\chi''(T)$ occurs at $\sim$11 K (T_c) which is less than half the value of the critical temperature seen in this virtually identical compound ($T_c = 24$ K), $Cr^{III}[Mn^{III}(CN)_6]\cdot 0.10MeCN$ (**3**). The difference in T_c between these two samples is likely caused by the different amount of defects afforded by the different synthetic routes. In **3**, building blocks with metals in the oxidation state of purely III were used (i.e., $[Cr^{III}(NCMe)_6]^{3+}$ and $[Mn^{III}(CN)_6]^{3-}$) where electron transfer does not occur to form $Cr^{III}[Mn^{III}(CN)_6]\cdot 0.10MeCN$ product. On the other hand, in the previously reported synthesis of $Cr^{III}[Mn^{III}(CN)_6]$, $[Cr^{II}(NCMe)_6]^{2+}$ and $[Mn^{IV}(CN)_6]^{2-}$ were used, and electron transfer is required. In the latter case because of the electron transfer between Cr^{II} and Mn^{IV}, local spin defects may lead to an incomplete electron transfer causing defect sites. These local spin defects will result in overall structural defects and as a result will ultimately decrease the T_c value of the compound. In the former case, where no electron transfer is needed, spin defects cannot occur.

The 2 K $M(H)$ data does not saturate at 90 kOe where a magnetization value of 5260 emu·Oe/mol is observed (Figure 5). At low temperature, with the spins in this system being antiferromagnetically coupled (for Cr^{III}, $S = {}^3/_2$ and $g = 2$; and for Mn^{III}, $S = 1$ and $g = 2.48$), a saturation magnetization value of 2903 emu·Oe/mol is expected. The observed value of 5260 emu·Oe/mol is substantially higher than the expected value. This is in accord with large structural disorder (seen in PXRD and ac susceptibility measurements) resulting an overall uncompensation of the spins. Nevertheless, hysteresis was observed for **3** at 2 K (H_{cr} value of 375 Oe) with a M_{rem} value of 430 emu·Oe/mol (Figure 6). This coercive field is the second largest for this $Cr[M(CN)_6]$ series and is caused by the structural disorder of the material.

The data above is consistent with **3** being a spin- or cluster-glass material with $T_f = 19$ K; however, bulk magnetic response is observed at a slightly higher critical temperature, T_c, of 24 K (ac data). The glassy behavior observed for **3** is a consequence of the compound being amorphous and structurally disordered and is confirmed by PXRD and several magnetic analyses. The data for compound **3** falls within the range of other reported critical temperatures of hexacyanomanganate(III)-based PBAs with T_c's ranging 22 to 31 K.[15,44,45]

Compound 4. Compound **4** has a room temperature χT value of 1.70 emu·K/mol, which is slightly lower than the spin-only value of 1.99 emu·K/mol (Cr^{III}, $S = {}^3/_2$ and $g = 2$; for Cr^{IV}, $S = 1$ and $g = 2$; for Fe^{II}, $S = 0$; and for Fe^{III}, $S = {}^1/_2$ and $g = 2.64$). Above 50 K, $\chi(T)$ was fit to the Curie−Weiss expression with $\theta = -12$ K, indicating antiferromagnetic coupling in the short-range exchange. With the use of this θ value, the $\chi T(T-\theta)_{calc}$ value is 1.92 emu·K/mol; however, the observed χT value is still slightly lower. As the temperature is lowered, the $\chi T(T)$ value gradually decreases to a minimum of 1.48 emu·K/mol at 30 K and then begins to increase. At 20 K, the $\chi T(T)$ value increases more rapidly, indicative of magnetic ordering, reaching a maximum of 2.32 emu·K/mol at 5 K (Figure 2). The minimum in $\chi T(T)$ above the ordering temperature is characteristic of a ferrimagnet. The overall low magnitude of magnetic ordering can be explained by the presence of significant amounts of diamagnetic ($S = 0$) $[Fe^{II}(CN)_6]^{4-}$, which decreases the number of nearest neighbors with nonzero spin states. Magnetic ordering has been reported for PB ($T_c = 5.5$ K)[46] and other PBAs,[47] of which the presence of diamagnetic ($S = 0$) $[Fe^{II}(CN)_6]^{4-}$ spin sites is observed. Nevertheless, **4** exhibits ferrimagnetic behavior, and $\chi^{-1}(T)$ was fit to eq 6[41] with $T_N = 10$ K. A θ value of -12 K was also obtained, which was

(44) Kurtz, W.; Babel, D. *Solid State Commun.* **1983**, *48*, 277.

(45) Entley, W. R.; Girolami, G. S. *Inorg. Chem.* **1994**, *33*, 5165.
(46) Ito, A.; Suenaga, M.; Ôno, K. *J. Chem. Phys.* **1968**, *48*, 3597.
(47) Sato, O.; Iyoda, T.; Fujishima, A.; Hashimoto, K. *Science* **1996**, *272*, 704. Matsuda, T.; Tokoro, H.; Hashimoto, K.; Ohkoshi, S. *Dalton Trans.* **2006**, 5046.

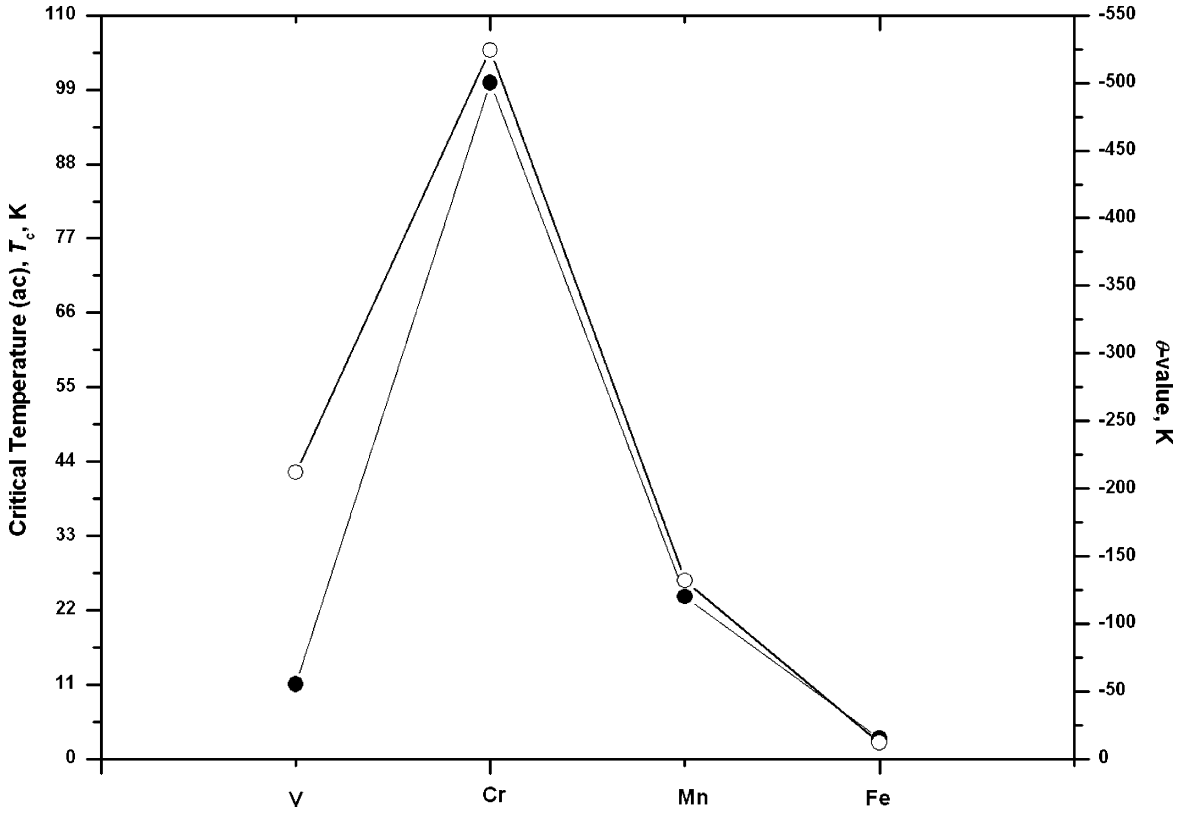

Figure 7. Periodic trends for the T_c's (●) and θ-values (○) for Cr[M(CN)$_6$] (M = V, Cr, Mn, Fe).

identical to the θ value fit from the high-temperature Curie−Weiss law. Literature θ values range from −8 to +23 K, and the type of coupling (ferro- to antiferromanetic) depends on the electronic configuration of the metals involved in the magnetic exchange.[25,48]

Low-field $M_{ZFC}(T)/M_{FC}(T)$ of **4** show the onset of magnetic ordering, T_{onset}, below 6 K and a blocking (irreversibility) temperature, T_b, of 5 K (Figure 3). The difference between the $M_{ZFC}(T)/M_{FC}(T)$ data is small, suggesting that the magnetic ordering in this sample is quite weak, consistent with the $\chi T(T)$ data. Although the coupling is weak, **4** exhibits weak ferrimagnetic ordering at low temperature.

The ac data shows a response in both the $\chi'(T)$ and $\chi''(T)$ data, and ferrimagnetic ordering was determined to occur with a T_c value of 3 K (initial rise in $\chi''(T)$ data on cooling) (Figure 4). This critical temperature is consistent with the blocking temperature obtained in the $M_{ZFC}(T)/M_{FC}(T)$ data, below which **4** is magnetically ordered. **4** has the largest frequency dependence of this Cr[M(CN)$_6$] family with ϕ = 0.040. This ϕ value is consistent with spin- or cluster-glass behavior,[42] and as stated above, this glassy behavior has been reported for other PBAs and can be attributed to the sample being a disordered and/or amorphous material.[16,43] Structural disorder was confirmed by PXRD of **4**; therefore, the sample was concluded to be amorphous (vide supra). The freezing temperature, T_f, of **4** is 2.5 K, which is consistent with the blocking temperature from the $M_{ZFC}(T)/M_{FC}(T)$ data. A frequency dependence in the ac data is expected and observed for this sample due to the substantial amount of structural (amorphous solid, PXRD) and spin (presence of paramagnetic Cr^{III} ($S = {}^3/_2$), Cr^{IV} ($S = 1$), and Fe^{III} ($S = {}^1/_2$) as well as the diamagnetic Fe^{II} ($S = 0$) atoms) disorder.

The 2 K $M(H)$ data show that **4** is almost saturated at 90 kOe where the magnetization value of 10 510 emu·Oe/mol is observed (Figure 5). At low temperature, with the antiferromagnetically coupled Cr and Fe spins (Cr^{III}, $S = {}^3/_2$ and $g = 2$; for Cr^{IV}, $S = 1$ and $g = 2$; and for Fe^{III}, $S = {}^1/_2$ and $g = 2.64$), this leads to an expected saturation magnetization of 10 770 emu·Oe/mol. The magnetization of **4** at high field approaches a saturation magnetization in accord with the $(NEt_4)_{0.04}Cr^{III}_{0.64}Cr^{IV}_{0.40}[Fe^{II}(CN)_6]_{0.40}[Fe^{III}(CN)_6]_{0.60}(BF_4)_{0.16}$·1.02MeCN formulation suggested by the ambient and low-temperature Mössbauer spectroscopy results. Hysteresis was observed at 2 K (H_{cr} of 17 Oe) with a M_{rem} value of 10 emu·Oe/mol (Figure 6).

The above data is consistent with **4** being a ferrimagnet (T_c of 3 K) with a cluster-glass behavior. The glassy behavior is a consequence of the compound being amorphous and structurally/spin disordered, which is confirmed by PXRD. Other hexacyanoferrate-based PBAs have numerous magnetic ordering temperatures ranging from below 2 to as high as 25 K.[25,28,32b,44,48]

Conclusion

The nonaqueous solvated Cr^{III} ion, $[Cr^{III}(NCMe)_6]^{3+}$, is substitionally more labile than its aqueous counterpart, $[Cr^{III}(OH_2)_6]^{3+}$. This was exploited to prepare a new family of PB-type magnets possessing Cr^{III} bound to the nitrogen end

(48) Egan, L.; Kamenev, K.; Papanikolaou, D.; Takabayashi, Y.; Margadonna, S. *J. Am. Chem. Soc.* **2006**, *128*, 6034.

of the bridging cyanides, $Cr[M(CN)_6]$ (M = V (**1**), Cr (**2**), Mn (**3**), Fe (**4**)). Antiferromagnetic coupling is observed for this PBA family, and the strength of coupling ranges from very strong ($\theta = -524$ K, for **2**) to weak ($\theta = -12$ K, for **4**). The antiferromagnetic coupling arises from the interactions of spins in nonorthogonal orbitals (i.e., $t_{2g}-t_{2g}$). Small antiferromagnetic coupling ($\theta = -12$ K) is observed for M = Fe (**4**) and is attributed to a reduced amount of $S = {}^1/_2$ $[Fe^{III}(CN)_6]^{3-}$ being available to couple to the $S = {}^3/_2$ Cr^{III} ions, and this is due to partial electron transfer forming $S = 0$ $[Fe^{II}(CN)_6]^{4-}$ and $S = 1$ Cr^{IV} in the solid state. In **3**, $[Mn^{III}(CN)_6]^{3-}$ has a $S = 1$ spin state interacting with the $S = {}^3/_2$ Cr^{III} ions, which increases the antiferromagnetic coupling ($\theta = -132$ K). For **2**, the spin is maximized in the series as $[Cr^{III}(CN)_6]^{3-}$ has a $S = {}^3/_2$ spin state, ultimately resulting in the strongest overall antiferromagnetic coupling of this family ($\theta = -524$ K). Finally, in **1**, the spin state of $[V^{III}(CN)_6]^{3-}$ is reduced to $S = 1$ and results in a decrease in the overall antiferromagnetic coupling ($\theta = -212$ K). This trend is displayed in Figure 7 and follows the general trend of other PB magnets where the strongest antiferromagnetic coupling is observed in the early first-row transition metals (i.e., V, Cr, and Mn).[1,5−8] From mean field theory[49] the magnetic ordering temperature, T_c, is directly proportional to the product of the exchange coupling (J) and $S(S + 1)$; therefore, the stronger the coupling the higher the T_c in a given family of compounds. Qualitatively, this trend is seen in **1**−**4** (Figure 7), and the highest T_c occurs when antiferromagnetic exchange coupling is the largest in **2**. The only compound that is at variance is **1**, which has a large antiferromagnetic coupling ($\theta = -212$ K), but the T_c value is relatively low. The low T_c value in **1** can be explained by large structural disorder that is supported by **1** having a structurally amorphous nature (PXRD) and the formation of ferrimagnetic domains that are separated by a sea on paramagnetic spins.

Thus, the substitionally more labile $[Cr^{III}(NCMe)_6]^{3+}$ can be used in the design and synthesis of new Prussian blue-type magnets. We are currently investigating incorporating Cr^{III} into other PB-type systems as well as other materials where the use of the kinetically inert $[Cr^{III}(OH_2)_6]^{3+}$ was an ineffective building block.

Acknowledgment. The authors gratefully acknowledge the continued partial support of the U.S. DOE Basic Energy Sciences (Grant No. DE FG 03-93ER45504) and the AFOSR (Grant No. F49620-03-1-0175).

Supporting Information Available: Figures S1−S5. This material is available free of charge via the Internet at http://pubs.acs.org.

IC7008489

(49) Carlin, R. In *Magnetochemistry*; Springer-Verlag: New York, 1986. Smart, J. S. In *Effective Field Theories of Magnetism*; W. B. Saunders: Philadelphia, PA, 1966.